VILNIUS UNIVERSITY

Gedmantė
RADŽIUVIENĖ

Assessment of sources of variation in *HER2* oncogene amplification and expression

SUMMARY OF DOCTORAL DISSERTATION

Natural Sciences,
Biology (N 010)

VILNIUS 2022

This dissertation was written between 2012–2015 and 2020–2021 at the National Center of Pathology, Affiliate of Vilnius University Hospital Santaros Klinikos, and at the Institute of Biosciences, Life Sciences Center, Vilnius University.

The research was supported by the Research Council of Lithuania.

Academic supervisor:
Prof. Dr. Arvydas Laurinavičius (Vilnius University, Medicine and Health Sciences, Medicine, M 001).
Academic consultant:
Prof. Habil. Dr. Juozas Rimantas Lazutka (Vilnius University, Natural Sciences, Biology, N 010).

This doctoral dissertation will be defended in a public/closed meeting of the Dissertation Defence Panel:

Chairman – **Dr. Vita Pašukonienė** (National Cancer Institute, Natural Sciences, Biology, N 010).
Members:
Prof. Dr. Jolanta Gulbinovič (Vilnius University, Medicine and Health Sciences, Medicine, M 001).
Prof. Habil. Dr. Dalia Pangonytė (Lithuanian University of Health Sciences, Natural Sciences, Biology, N 010).
Dr. Linas Petkevičius (Vilnius University, Natural Sciences, Informatics, N 009)
Prof. Dr. Darren Treanor (University of Leeds, United Kingdom, Medicine and Health Sciences, Medicine, M 001).

The dissertation shall be defended at a public meeting of the Dissertation Defence Panel at 2 pm on 30th of September 2022, in auditorium R-103 of Life Sciences Center of Vilnius University (address: Saulėtekio Ave. 7, LT-10257, Vilnius, Lithuania) and/or remotely.

The text of this dissertation can be accessed at the library of Vilnius University as well as on the website of Vilnius University:
www.vu.lt/lt/naujienos/ivykiu-kalendorius

VILNIAUS UNIVERSITETAS

Gedmantė
RADŽIUVIENĖ

HER2 onkogeno amplifikacijos ir raiškos variacijos šaltinių nustatymas

DAKTARO DISERTACIJOS SANTRAUKA

Gamtos mokslai,
Biologija (N 010)

VILNIUS 2022

Disertacija rengta 2012–2015; 2020–2021 metais Valstybiniame patologijos centre, Vilniaus universiteto ligoninės Santaros klinikų filiale, ir Biomokslų institute, Gyvybės mokslų centre, Vilniaus universitete.

Mokslinius tyrimus rėmė Lietuvos mokslo taryba.

Mokslinis vadovas:
prof. dr. Arvydas Laurinavičius (Vilniaus universitetas, medicinos ir sveikatos mokslai, medicina, M 001).
Mokslinis konsultantas:
prof. habil. dr. Juozas Rimantas Lazutka (Vilniaus universitetas, gamtos mokslai, biologija, N 010).

Gynimo taryba:
Pirmininkė – dr. Vita Pašukonienė (Nacionalinis vėžio institutas, gamtos mokslai, biologija, N 010).
Nariai:
prof. dr. Jolanta Gulbinovič (Vilniaus universitetas, medicinos ir sveikatos mokslai, medicina, M 001).
prof. habil. dr. Dalia Pangonytė (Lietuvos sveikatos mokslų universitetas, gamtos mokslai, biologija, N 010).
dr. Linas Petkevičius (Vilniaus universitetas, gamtos mokslai informatika, N 009).
prof. dr. Darren Treanor (Lidso universitetas, Jungtinė Karalystė, medicinos ir sveikatos mokslai, medicina, M 001).

Disertacija ginama viešame Gynimo tarybos posėdyje 2022 m. rugsėjo mėn. 30 d. 14 val. Vilniaus universiteto Gyvybės mokslų centre, R-103 auditorijoje (adresas: Saulėtekio alėja. 7, LT-10257, Vilnius, Lietuva) ir/arba nuotolinius būdu.

Disertaciją galima peržiūrėti Vilniaus universiteto bibliotekoje ir VU interneto svetainėje adresu: *https://www.vu.lt/naujienos/ivykiu-kalendorius*

CONTENT

ABBREVIATIONS

ASCO – American Society of Clinical Oncology/College of American Pathologists
AshD – Ashman's D
CAP – College of American Pathologists
CEP17 – centromere enumeration probe for chromosome 17
CI – confidence interval
CM – center of mass
DAPI – fluorescence dye (*4',6-Diamidino-2-Phenylindole, Dilactate*)
DIA – digital image analysis
ER – estrogen receptor
FISH – fluorescence *in situ* hybridization
FFPI – formalin-fixed paraffin-embedded
G – histological grade
HER2 – the human epidermal growth factor receptor 2
HR – hazard ratio
ID – immunodrop
IHC – immunohistochemistry
IZ – interface zone
LR – likelihood ratio
N – lymph node metastasis status
OS – overall survival
PR – progesterone receptor
T – tumor stage
TE – tumor edge
TIL – tumor infiltrating lymphocyte
WSI – whole slide image

INTRODUCTION

Relevance of the Study

Breast cancer is the most frequently diagnosed malignancy among females in Lithuania and in most countries in the world (1, 2).

Advance of medicine and science, as well as screening and prevention programs, are improving the diagnosis and treatment of breast cancer; however, morbidity and mortality from this disease remain high (3). New treatment options emerged in recent decades, including targeted therapy and imunotherapy, provide opportunities to further improve treatment of cancer patients.

Breast cancer is a complex and diverse disease with distinct clinical, pathological, and molecular characteristics. The multifaceted nature of the disease leads to diverse clinical outcomes and therapeutic responses. Current clinical practice of breast cancer prognosis and treatment selection is based on clinical and pathology parameters – tumor size (T), lymph node status (N), histological grade (G), and expression of biomarkers – estrogen receptor (ER), progesterone receptor (PR), human epidermal growth factor receptor 2 (HER2) status (4). However, these criteria are insufficient for personalized clinical decisions in breast cancer patients (5). Therefore, novel prognostic breast cancer biomarkers are intensively searched and investigated (6).

Amplification and/or overexpression of *HER2* oncogene is observed in approximately 15–20% of breast cancer (7, 8). These HER2-positive tumours are characterized by highly aggressive course with poor prognosis. Therefore, robust biomarkers are in demand to improve selection of the patients for current and emerging therapies of HER2-positive metastatic breast cancer (9) as well as to predict resistance for anti-HER2 therapies (10) and recurrence of the disease (11). HER2 is not only a prognostic marker but also an important target for biological therapy: the monoclonal antibody trastuzumab (Herceptin; Genentech, South San Francisco, USA) used to treat

HER2-positive breast cancer more than two decades ago prevents disease progression and significantly prolongs patient survival (12-14). Accurate detection of HER2 status is thus essential for individual therapy decisions .

Nevertheless, even after decades of extensive HER2 testing in breast cancer based on standardized methodologies and on the evidence from clinical studies to select patients for HER2 target therapy, important questions remain unanswered in the HER2 testing. While the majority of tumors can be categorized as either HER2-positive or HER2-negative by IHC and in situ hybridization (ISH) techniques, regarded as the standard methods to assess HER2 status in breast cancer (15), the analysis of borderline tumors remains problematic. These tumors are often heterogeneous, with an increased copy number of the chromosome 17 centromere (CEP17), contributing to interobserver disagreement and, most importantly, posing therapeutic dilemmas (16-20). The challenges in interpretation of HER2 borderline tumors accounting for up to 18% of breast cancers are reflected by multiple revisions of the definitions and criteria by the American Society of Clinical Oncology/College of American Pathologists (ASCO/CAP) HER2 guidelines (15, 21, 22).

The phenomenon of the intratumoral heterogeneity of HER2, at both protein expression and gene amplification levels, present a potential source of variation in the assessment of HER2 status in borderline cases. Potential discrepancies in the results from the IHC and fluorescence *in situ* hybridization (FISH) techniques may futher complicate the assessment of HER2 status and lead to inadequate treatment selection and response to it (16, 23, 24). To address an issue of *HER2* heterogeneity, the genetic heterogeneity definition was proposed (25); however, it was criticized because of the lack of evidence-based data regarding the frequency and clinical relevance and significance of genetic heterogeneity (23, 26-28). Subsequently, the definition of genetic heterogeneity was refocused from individual cells to a discrete population of tumor cells (22), the method of genetic heterogeneity assessment is still based on visual analysis of a limited

number of cells, which may be not representative of actual intratumoral variance of the HER2 amplification status. Also, the guidelines for assessment of intratumoral HER2 IHC heterogeneity are lacking. The semi-quantitative HER2 IHC method limits the ability to measure the diversity of individual cells or areas in the tumor tissue, although tumors evaluated with a single value may consist of heterogeneous areas. Therefore, an objective and reliable methodology for assessing the intratumoral heterogeneity phenomenon at both HER2 protein and gene levels, as well as the variable expression of hormone receptors, is in particular demand.

The changes of CEP17 copy number (increase or decrease) is another significant source of variation in interpreting *HER2* FISH results (19, 29). It can be responsible for misleading results, especially in borderline cases, therefore an accurate and objective assessment of the CEP17 copy number variation is also important.

Recent advances in cancer immunotherapy options shifted the focus towards research on local immune response in the context of tumor microenvironment, including breast cancer patients (30, 31). Presence of tumor infiltrating lymphocytes (TILs) has been associated with a better prognosis in various solid tumors; however the data are conflicting in different breast cancer subtypes (32, 33). Relative prognostic impact of TILs and other features of the tumor, including HER2 status, remains to be elucidated in bordeline HER2 breast cancer, taking the advantage of novel digital image analysis (DIA) methods that generate high-capacity data, including spatial aspects of intratumoral distribution of the biomarkers.

The Aim of the Study

To assess the sources of variation in *HER2* oncogene amplification and expression and explore the prognostic indicators by digital image analysis methods in the group of breast cancer patients with bordeline HER2 protein expression.

The Objectives of the Study

1. To automate the evaluation of *HER2* gene status by FISH using digital image analysis algorithms and compare to the results of routine visual assessment.
2. To assess the intratumoral variance of *HER2* and CEP17 copy numbers from FISH digital image analysis data and its impact on *HER2* FISH test results.
3. To measure the intratumoral heterogeneity of HER2, ER, PR, and Ki67 expression in breast cancer tissue using digital image analysis and explore their prognostic value in the tumors with borderline HER2 expression.
4. To explore prognostic value of indicators based on spatial distribution of CD8+ lymphocytes in the tumor microenvironment of HER2 borderline breast cancer in the context of other prognostic features of the disease.

Statements to be Defended

1. High-capacity analysis of *HER2* FISH digital images provides new opportunities to quantify intratumoral heterogeneity of *HER2* gene amplification in breast cancer tissue.
2. Intratumoral heterogeneity indicators of IHC biomarkers can serve as independent predictors of overall survival (OS) of breast cancer patients with borderline HER2 protein expression.
3. CD8+ cell density indicators in the tumor–stroma interface zone (IZ) of breast cancer tissue are independent prognostic factors of

overall survival of the breast cancer patients with established borderline HER2 protein expression.

The Scientific Novelty of the Study

The methods of DIA and computational analytics, applied in this study, revealed novel aspects of HER2 amplification and expression, taking into account their intratumoral heterogeneity, to further optimize tissue diagnostics and discover independent prognostic factors in HER2 IHC borderline (IHC 2+) breast cancer patients.

For the first time, automated FISH analysis algorithms were applied to investigate *HER2* gene expression heterogeneity. The study presents digital data-driven and quantifiable measures of *HER2* intratumoral heterogeneity (bimodality), based on *HER2* signal variance in breast cancer cells. The bimodality indicators, beeing linearly independent of the level of *HER2* amplification and increased CEP17 copy number, can be used for definitions of intratumoral heterogeneity in HER2 IHC 2+ tumors to supplement the current *HER2* genetic heterogeneity concept, which is confined an assessment of a limited number of cells.

The intratumoral heterogeneity of HER2 protein and other standard breast cancer IHC biomarkers - ER, PR, and Ki67 expression in the tumor tissue was quantitatively measured using DIA and hexagonal grid subsampling of the DIA outputs. Comprehensive intratumoural heterogeneity analysis of these biomarkers in the context of bordeline HER2 protein expression has not been performed previously. Our methods allowed to discover independent prognostic indicators, representing intratumoural heterogeneity of HER2 and ER IHC expression, that supplement the clinical and pathological parameters of breast cancer and outperform other quantitative indicators used for the assessment of the IHC biomarkers.

We applied novel computational method of IZ immunogradient (34) which revealed independent prognostic factors of OS based on indicators of CD8+ lymphocyte distribution in the breast cancer

microenvironment. In the *HER2* non-amplified group, three independent computational biomarkers, representing CD8+ cell density, density profile across the IZ, and density variance along the IZ, were sufficient to predict OS without contribution of clinicopathological variables. Remarkably, a combined score based on these three computational biomarkers, obtained from a single CD8 IHC image, further enhanced risk stratification of the patient OS. Data from previous studies of the prognostic value of CD8+ lymphocytes in both the *HER2* non-amplified (hormone receptor-positive) and amplified tumors are controversial (33, 35).

1. MATERIALS AND METHODS

1.1. Study Population and Design of the Study

Fifty female patients with invasive ductal breast carcinoma diagnosed as borderline HER2 IHC (2+) and assessed *HER2* gene status by FISH, treated at the National Cancer Institute (Vilnius, Lithuania), and investigated at the National Center of Pathology (Vilnius University Hospital Santaros Klinikos, Vilnius, Lithuania) between September 2012 and February 2015 were selected for retrospective digtal imge analysis of *HER2* gene status.

For comprehensive digital image analysis of breast cancer IHC (ER, PR, HER2, Ki67) and CD8 biomarkers, the initial cohort (n = 50) was supplemented with the cases of invasive ductal breast carcinoma with the assessed borderline HER2 IHC (2+) and *HER2* gene status (n = 252) collected between September 2012 and March 2017. The cases without paraffin blocks available for ER, PR, Ki67, CD8 IHC staining and DIA, and without available follow-up data were excluded (15 and 12 cases, respectively). The final cohort included 275 patients which was split into the *HER2* non-amplified (*HER2*/CEP17 ratio < 2; average *HER2* copy number < 2 signals per cell) and amplified (*HER2*/CEP17 ratio ≥ 2.0; average *HER2* copy number ≥ 4.0 signals per cell) groups (15). All the cases (n = 59, 37.3%) which were FISH equivocal (*HER2*/CEP17 ratio < 2; average *HER2* copy number ≥ 4 and < 6 signals per cell) under the 2013 guidelines (22) were reclassified into *HER2* non-amplified according to the 2018 guidelines (15).

The study was approved by the Lithuanian Bioethics Committee (reference number: 40, April 26, 2007, updated on March 18, 2013, and on July 4, 2016).

The clinicopathological and follow-up characteristics are summarized in Table 1.

Table 1. Patient and tumor characteristics according to HER2 status

Characteristic	**Total**	***HER2* non-amplified group, n (%)**	***HER2*-amplified group, n (%)**	***p*-Value***
Number of patients	275	158 (57.5)	117 (42.5)	-
Median age, years (range)	60 (29-92)	59 (33-86)	63 (29-92)	0.2247
Follow up, months				
Median (range)	58 (0.7-102)	64 (2-102)	52 (0.7-100)	-
Deceased	42	22 (13.7)	20 (17.1)	-
Histological grade (G)				
G1	22	18 (11.4)	4 (3.4)	<0.0001*
G2	153	99 (62.7)	54 (46.2)	
G3	100	41 (25.5)	59 (50.4)	
Tumor invasion (T)				
T1	129	77 (48.7)	52 (44.4)	0.7578
T2	129	73 (46.2)	56 (47.9)	
T3	9	4 (2.5)	5 (4.3)	
T4	8	4 (2.5)	4 (3.4)	
Lymph node mestastasis (N)				
N0	166	96 (60.8)	69 (59)	0.3225
N1	66	41 (26)	25 (21.4)	
N2	30	16 (10.1)	14 (12)	
N3	14	5 (3.2)	9 (7.7)	
Metastasis (M)				
M0	272	156 (98.73)	116 (99.15)	0.9999
M1	3	2 (1.27)	1 (0.85)	

HER2 - human epidermal growth factor receptor 2; variables were cmpared using Chi-square test or Fisher's exact test; *p-Value < 0.05 is considered significant.

1.2. Fluorescence *In Situ* Hybridization

4 µm-thick sections were stained with PathVysion *HER2* DNA Probe Kit (Abbott-Vysis, Inc., USA) following the manufacturer's instructions. In this kit, a fluorescently labeled (SpectrumOrange) DNA probe recognizing the *HER2* locus (17q11.2-q12) is used in conjunction with a fluorescently labeled (SpectrumGreen) DNA probe recognizing the centromeric region of CEP17 (17p11.1-q11.1).

The microscopic and digital analysis of samples was performed using a fluorescence microscope (Zeiss, Axio Imager.Z2, Germany) equipped with single-pass filters for DAPI, HER2, and CEP17, under a 63× oil immersion objective. HER2 status was determined according to 2013 ASCO/CAP guideline (22) and re-determined according to 2018 updated guideline (15). Two observers evaluated the mean number of *HER2* and CEP17 signals and the *HER2*/CEP17 ratio per nucleus by conventional manual procedure (MP): 40 nuclei were examined in two or more fields; for equivocal cases, additional 20 nuclei were evaluated. *HER2*/CEP17 ratios were calculated per tumor by total number of *HER2* signals divided by total number of CEP17.

HER2 amplification status was determined according to the ASCO/CAP (15, 22).

The *HER2* genetic heterogeneity was estimated by (1) the ASCO/CAP 2009 guidelines (defined as the presence of more than 5% but less than 50% of infiltrating tumor cells with a *HER2*/CEP17 ratio > 2.2 when using a control probe or > 6 *HER2* signals per cell when using a probe for *HER2* only) (25), which were applied to both MP and automatically detected data (AD) to compare the effect of number of included nuclei on the heterogeneity measure and (2) statistical bimodality indicators: Ashman's D (AshD) and bimodality index. Briefly, bimodality indicators are functions of the parameters describing two Gaussian distributions fitted to the data (36). The bimodality indicators were calculated for AD distributions of *HER2*, CEP17, and HER2/CEP17 ratio as extracted per cell by DIA.

The bimodality is detected when AshD > 2.

CEP17 polysomy was defined as an average CEP17 copy number ≥ 3 (37).

1.3. Acquisition and analysis of digital *HER2* FISH images

TissueFAXS-plus (TissueGnostics, Austria) scanning system was used to scan representative regions of the samples. Acquisition of digital images was performed by 63x/1.4 oil objective and the single

band-pass filters were fitted to record nuclei (DAPI), HER2 (Acridine), and CEP17 (FITC) in separately. Each region consisted of a minimum of 4 field of views (FOVs). Digital images were stitched together to regions of interest (ROIs). Each FOV was stored at the resolution of 1392 by 1024 pixels, yielding a pixel size of 0.16 μm. To ensure that all signals inside the thick tissue section are available for DIA, images were acquired using z-stacks composed of 9 steps with a step size of 0.45 μm. Extended depth of focus algorithm of TissueFAXS was used to combine the multiple focal planes. The algorithm is using only the sharpest structures of each layer.

ROIs were manually selected for the scanning. Automated segmentation of both nuclei and FISH signals was performed with StrataQuest v.205 (TissueGnostics, Austria). All automatically detected nuclei, HER2 and CEP17 signals were reviewed and edited by the observer (Gedmante Radziuviene) on the digital images to produce a set of corrected data (CD) for quality assurance. All nuclei were considered. Subsequently, nuclei without the FISH signals or with only one HER2 or CEP17 signal were excluded from further statistical analyses.

1.4. Immunohistochemical staining

Formalin-fixed paraffin-embedded (FFPE) tissue sections were cut at 3 μm thickness and mounted on positively charged slides. IHC staining was performed by a Roche Ventana BenchMark ULTRA automated slide stainer (Ventana Medical Systems, USA). IHC for ER, PR, and HER2 was performed using ready-to-use antibodies (SP1, 1E2, and 4B5, respectively, Ventana (USA)); for Ki67 and CD8 – MIB-1, Dako (Denmark; dilution 1:100) and C8/144B, Dako (Denmark; dilution 1:100) antibodies, respectively. Visualization of ER, PR, Ki67, HER2, and CD8 was performed with the ultraView Universal DAB Detection kit (Ventana Medical Systems, USA). The sections were counterstained with Mayer's hematoxylin.

1.5. Acquisition and analysis of IHC images and calculation of indicators

ER, PR, Ki67, HER2 IHC slides were scanned using a ScanScope XT Slide Scanner (Leica Aperio Technologies, USA), and CD8 IHC slides using an Aperio AT2 Slide Scanner (Leica Biosystems, USA**)** at 20× magnification (0.5 μm per pixel).

The DIA was performed on the whole slide images (WSI) with HALO software (version 3.0311.174; Indica Labs, USA). The tissue was classified into the tumor, stroma and background (consisting of glass, necrosis and artifacts) by HALO AI classifier. Then, the HALO Multiplex IHC algorithm (version 1.2) was applied to obtain coordinates of ER, PR, Ki67, CD8 cells and Membrane algorithm (version 1.4) - of HER2 cells in the IHC WSI. For quality assurance, all image analysis results were approved by the pathologist.

For subsequent analysis the following IHC indicators obtained by DIA were used: positive cell percentages for ER, PR, Ki67 and CD8 and the percentages of HER2 2+ and 3+ cells along with the cell membrane completeness indicator.

The hexagonal tiling methodology was applied to calculate the spatial tumor texture and intratumoral heterogeneity indicators of biomarkers expression as previously reported (38). Briefly, the HALO DIA data were subsampled by a hexagonal grid - the cells were assigned to 825-pixel-sized hexagons (hexagon side length 257 μm) according to their extracted coordinates. Hexagons containing fewer than 50 cells were regarded as insufficient sampling and were not used for further analyses. The percentages of ER, PR, Ki67, and HER2-positive cells were calculated for each hexagon which was then ranked into 10 intervals (0–10%, >10–20%, etc.). Based on the ranks, a co-occurrence matrix was constructed to compute Haralick's texture indicators (contrast, dissimilarity, entropy, energy, and homogeneity) (39).

The bimodality indicator (AshD) to assess the intratumoral distribution of each IHC biomarker expression was calculated as described previously (40).

The distribution of CD8+ lymphocytes was measured at the automatically extracted tumor edge and tumour-stroma IZ. The method based on DIA tissue classification data and their subsampling into hexagonal grids is described in detail in (34).

An IZ of seven hexagon width (hexagon side length 65 μm) and TE of one hexagon width were used in the study. Quantitative CD8+ cell density indicators (the mean and standard deviation (SD)) were computed in both 1) the WSI stroma and tumor areas and 2) within the tumor–stroma IZ, which consists of stroma (S), tumor (T), and tumor edge (TE) aspects. Subsequently, two immunogradient indicators: center of mass (CM) and immunodrop (ID) reflecting CD8+ cell density change in the stroma-to-tumor direction were computed. The CM indicator reflects CD8+ cell density increase towards the tumor within the IZ, while the immunodrop indicator reflects an abrupt decrease of CD8+ cell density across the TE (IZ rank 0) from stroma (IZ rank −1) to tumor (IZ rank 1), represented by the CD8+ cell density ratio between rank −1 and rank 1.

1.6. Statistical analysis

Continuous variables (IHC, FISH, intratumoral heterogeneity, bimodality, CD8+ cell density and immunogradient indicators) were expressed as mean, SD and median, whereas categorical variables (clinicopathological indicators) - as absolute numbers and percentages.

All continuous variables were tested for normal distribution by Shapiro-Wilk or Kolmogorov–Smirnov tests. Parametric tests were used for normally distributed data and non-parametric tests - for asymetrically distributed data. A log-transformation was applied to normalize the asymmetric distributions of quantitative and spatial

variables of CD8+ cell density and to meet the assumptions of parametric statistical tests.

To assess the accuracy of the automatically detected *HER2* copy number, CEP17 copy number and *HER2*/CEP17 ratio were compared firstly to the corrected data, then to the data obtained by manual procedure using paired *t*-test.

Comparison of continuous variables between the groups (*HER2* non-amplified and amplified) was performed by two-tailed Student's *t*-test or by the Mann–Whitney *U* test. The CD8+ cell density variation in different aspects of the IZ was tested by one-way ANOVA followed by Bonferroni's post-hoc test for pairwise comparisons and a two-sided Welch's t-test for homogeneity of variances. The pairwise relationships between the quantitative variables were estimated by Pearson or Spearman correlation analyses. Chi-square test or Fisher's exact test were used to assess the differences of clinicopathological variables between the patient groups.

A factor analysis was performed using the factoring method based on principal component analysis; factors were retained based on the threshold of an eigenvalue of 1; a general orthogonal varimax rotation of the initial factors was applied. On the resulting factor scores in *HER2* FISH analysis, clusters were extracted by the k-Means method to explore potential stratification of the cases.

The optimal cutoff value for each indicator was determined using Cutoff Finder tool (41) to test the predictions of OS. The Kaplan–Meier method was applied to estimate the OS distributions with the log-rank test to compare survival differences between the stratified groups. To assess the prognostic factors, univariate and multivariate analyses were performed using the Cox proportional-hazards models. Cox regression models were validated using leave-one-out cross-validatation (42). All *p*-values were considered significant at the < 0.05 level. Statistical analyses were performed with SAS software (version 9.4; SAS Institute Inc., Cary, USA); plots were generated by R (version 4.1.0).

2. RESULTS

2.1. Digital *HER2* FISH image analysis

2.1.1. Comparison of automated, corrected and evaluated by manual procedure *HER2* FISH results

Overall, 155 *HER2* FISH digital images from 50 patients were analyzed. A total of 36,154 nuclei were detected, of which, 27,266 (75.4%) were correctly segmented, 5,626 (15.6%) were under- or over- segmented, and 3,262 (9.0%) were not detected. A range of 192 to 789 nuclei per tumor were evaluated by the DIA.

Overall, 87,092 *HER2* and 65,309 CEP17 signals were detected by the automated analysis. Among them, 81,704 (93.8%) *HER2* signals and 1,116 (96.6%) CEP17 signals were correctly detected, while 2,163 (2.5%) and 1,116 (1.7%) were falsely detected, and 3,225 (3.7%) and 1,115 (1.7%) were undetected, respectively.

No significant bias was found between the AD and CD for mean CEP17 copy number and negligible bias for mean *HER2* copy number and mean *HER2*/CEP17 ratio (data not shown). However, the manual *HER2*, CEP17 counts and *HER2*/CEP17 ratio were significantly underestimated by the automated procedure: average difference 1.428, CI (confidence interval) = [1.188; 1.668], $p < 0.0001$ for mean *HER2* copy number, average difference 0.580, CI = [0.483; 0.676], $p < 0.0001$ for mean CEP17 copy number and average difference 0.240, CI = [0.150–0.330], $p < 0.0001$ for *HER2*/CEP17 ratio.

2.1.2. Heterogeneity analysis of automatically evaluated *HER2* FISH data

HER2 FISH data underestimation by DIA had an impact on lower percentages of amplified cells (*HER2*/CEP17 ratio > 2.2) by automated compared to the manual procedures at different ranges: the percentages of amplified cells were lower in AD compared to MP (amp_%_A and amp_%_M, resp.) in the range above 25% by MP;

however, amp_%_A were higher (reaching up to 20%) than amp_%_M in the range below 5% by MP (Figure 1(a)).

The distribution of nonamplified, equivocal, amplified, and genetically heterogeneous cases evaluated by MP according to the ASCO/CAP guidelines (26, 29) is shown in Figures 1 (b) and 1 (c), respectively. A gap occured in the distribution of genetically heterogeneous cases which were detected only if they contained at least 28% of the amplified cells, but were not detected in the presence of 5 to 28% of the amplified cells (Figure 1 (c)). The effect of underestimation by AD is shown in Figure 1 (d): fewer cases being amplified or equivocal were detected as they were downgraded into the range for negative cases. This impact is also reflected in the distribution of amp_%_A; however, importantly, a continuous distribution of amplified cell percentages can be noted for AD shown in Figure 1 (e).

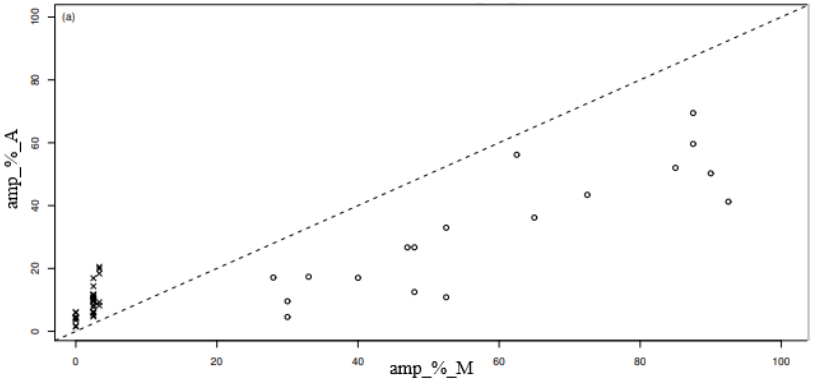

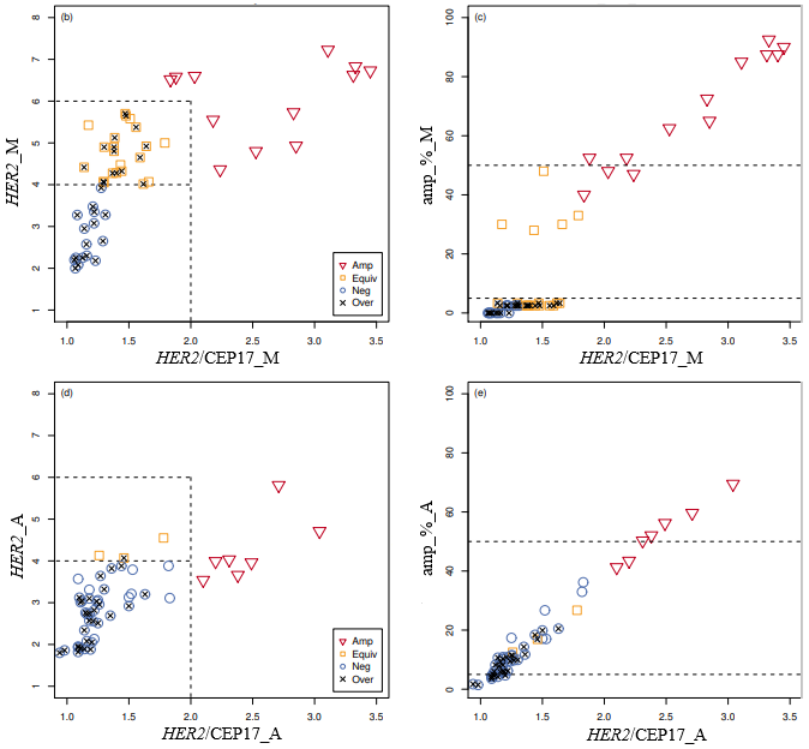

Figure 1. Distribution of tumors with regard to genetic heterogeneity and amplification guidelines. (a) Percentage of amplified cells plotted for MP and AD values, amp_%_M and amp_%_A, respectively. Dashed line marks identity line. AD overestimates low MP values (crosses) whereas it underestimates MP values in the range >28 (circles); (b) *HER2*_M plotted against *HER2*/CEP17_M with cut-offs for amplification by ASCO/CAP 2013 guidelines shown by grey lines. Cases marked with crosses are overestimated cases from (a); (c) amp_%_M plotted against *HER2*/CEP17_M, horizontal lines at 5% and 50% mark cut-off values for determining genetically heterogeneous cases. Note the lack of cases in the 3–28% range; (d) *HER2*_A plotted against *HER2*/CEP17_A, amplification cut-off marked in grey; (e) amp_%_A plotted against *HER2*/CEP17_A. Summary: MP: 13 amplified, 21 equivocal, 16 non-amplified, and 8 genetically heterogeneous cases; AD: 7 amplified, 3 equivocal, 40 non-amplified, and 36 genetically heterogeneous cases.

HER2 – human epidermal growth factor receptor 2; *HER2*_A, *HER2*/CEP17_A, *HER2*_M, *HER2*/CEP17_M – *HER2* copy number and *HER2*/CEP17 ratio detected by automated and manual procedures, respectively; amp_%_A, amp_%_M – percentage of amplified cells, calculated from *HER2*/CEP17 ratio and detected by automated and manual procedures, respectively.

2.1.3. Factor analysis of *HER2* FISH indicators

FISH data obtained by the manual and automated procedures (*HER2* and CEP17 copy number, *HER2*/CEP17 ratio, percentage of amplified cells, nuclei size) and bimodality parameters (*HER2*_AshD, CEP17_AshD, *HER2*/CEP17_AshD, *HER2*_BI, CEP17_BI, *HER2*/CEP17_BI) were included in factor analysis. The rotated factor pattern of the 3 factors was extracted (Figure 2).

Factor 1 was charazterized by strong positive loadings of the variables indicative of *HER2* amplification (including *HER2* counts, HER2/CEP17 ratios, and percentages of amplified cells by MP and AD) and was therefore interpreted as the amplification factor. Factor 2, which can be interpreted as representing an increased CEP17 copy number, was characterized by strong positive loadings of CEP17 copy number detected by MP and AD along with negative loading of bimodality index calculated for CEP17. Factor 3 was described by positive loadings of the bimodality indicators (mainly from AshD estimated from *HER2* and CEP17 distributions, less from the *HER2*/CEP17 data) and was named the bimodality factor.

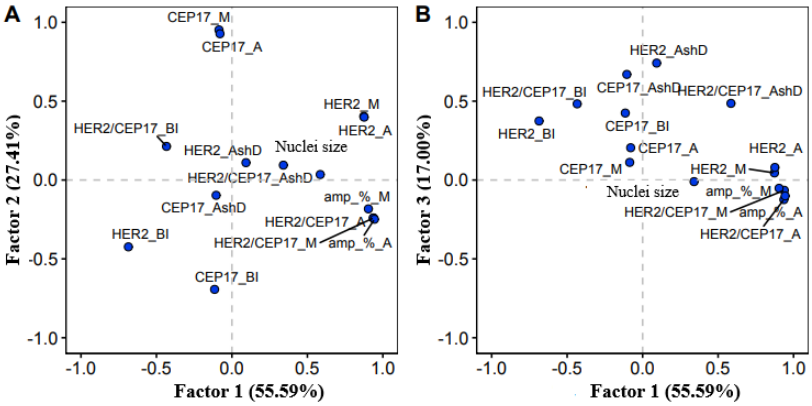

Figure 2. Rotated factor pattern of the indicators obtained by the manual and automated HER2 FISH procedure: The loadings of (A) factors 1 and 2, (B) factors 1 and 3.

HER2 – human epidermal growth factor receptor 2; CEP17 – centromere enumeration probe for chromosome 17; *HER2*_A, CEP17_A, *HER2*/CEP17_A – *HER2*, CEP17 copy number and *HER2*/CEP17 ratio detected by automated procedure, respectively; *HER2*_M, CEP17_M, *HER2*/CEP17_M – *HER2*, CEP17 copy number and *HER2*/CEP17 ratio detected by manual procedure, respectively; amp_%_A, amp_%_M - percentage of amplified cells, calculated from *HER2*/CEP17 ratio and detected by automated and manual procedures, respectively; *HER2*_AshD, CEP17_AshD ir *HER2*/CEP17_AshD – Ashman's D indicator calculated for *HER2*, CEP17 and *HER2*/CEP17 ratio automated data; *HER2*_BI, CEP17_BI and *HER2*/CEP17_BI – bimodality indicators calculated for *HER2*, CEP17 and *HER2*/CEP17 automated data.

2.1.4. Cluster analysis

Analysis of the factor score plots (Figures 3 (a - c) revealed potential nonlinear relationship between the amplification and an increased CEP17 copy number factors and potential clustering of the tumors. A cluster analysis of the 3 factor scores extracted 4 rather distinct clusters presented in Figure 4 and characterized in Table 2.

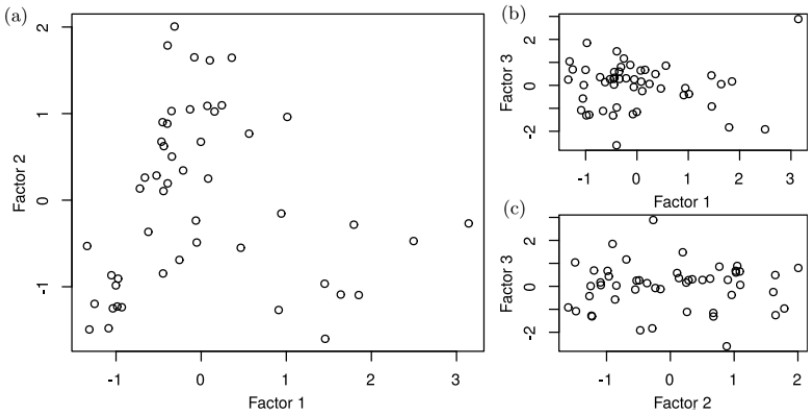

Figure 3. The factor score plots between: (a) factor 1 (amplification) and factor 2 (increased CEP17 copy number); (b) factor 1 and factor 3 (bimodality); (c) factor 2 and factor 3.

The clusters 1 and 2 (containing 1 and 9 cases, respectively) revealed variable degree of amplification and bimodality factor scores. Cluster 3 consisted of non-amplified tumors (18 cases); however, a significant proportion of them were characterized by a high HER2 bimodality score (33.3% cases with AshD > 2). Cluster 4 was mainly represented by tumors with equivocal and/or increased CEP17 copy numbers (22 cases).

Although it was possible to distinctly classify the tumors into amplified, non-amplified and equivocal/with increased CEP17 copy number types by cluster analysis, the bimodality factor was variable in all the clusters and provided an independent characteristic for the cell diversity.

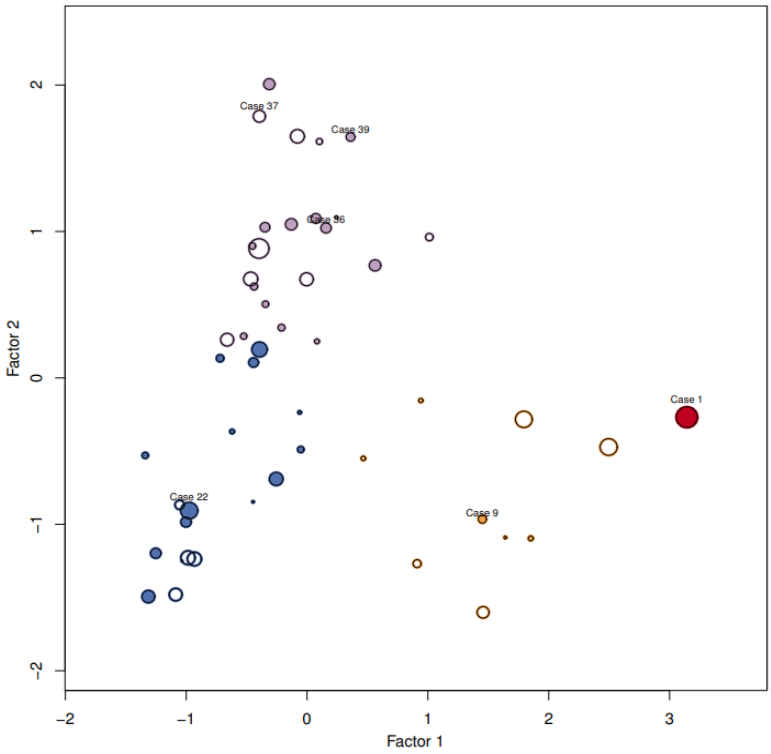

Figure 4. A bubble plot of the clusters obtained from the factor 1, 2, and 3 scores. Cluster colors: Cluster 1, red; Cluster 2, yellow; Cluster 3, blue; and Cluster 4, purple. Bubble size represents factor 3 (bimodality); center is empty for negative and filled for positive values.

Table 2. Characteristics of the clusters extracted from the automated image analysis data

	Cluster 1	Cluster 2	Cluster 3	Cluster 4	Total
No of observations	1 (2 %)	9 (18 %)	18 (36 %)	22 (44 %)	50
Amplifikacion in the cohort amp/equiv/neg	1 (2 %)/0/0	9 (18 %)/0/0	0/4 (8 %)/14 (28 %)	3 (6 %)/17 (34 %)/2 (4 %)	50
Amplifikacion in clusters amp/equiv/neg	1 (7.7 %)/0/0	9 (69.2%)/0/0	0/4 (19.1 %)/14 (87.5 %)	3 (23.1 %)/17 (80.9 %)/2 (12.5 %)	13/21/16
≥ 3 CEP17 copy number	0	0	3 (13.6 %)	19 (86.4 %)	22
GH (amp_%_M), (by *HER2*/CEP17 ratio)	0	1 (12.5 %)	1 (12.5 %)	6 (75 %)	8
GH (amp_%_M) (by *HER2* only)	0	4 (14.8 %)	6 (22.2 %)	17 (63 %)	27
HER2/CEP17_AshD > 2	1 (20 %)	1 (20 %)	2 (40 %)	1 (20 %)	5
*HER2*_AshD > 2	1 (4.3 %)	4 (17.4 %)	6 (26.1 %)	12 (52.2 %)	23
CEP17_AshD > 2	1 (9 %)	0	5 (45.5 %)	5 (45.5 %)	11
Predominantly	Amplified	Amplified	Non-amplified	Equivocal; ≥ 3 CEP17 copy number; Bimodal	

HER2 – human epidermal growth factor receptor 2; CEP17 – centromere enumeration probe for chromosome 17; GH – genetical heterogeneity; amp_%_M: percentage of amplified cells detected by manual procedure, calculated from *HER2*/CEP17 ratio and by *HER2* signal only. *HER2*_AshD, CEP17_AshD ir *HER2*/CEP17_AshD: Ashman's D indicator calculated for *HER2*/CEP17, *HER2* and CEP17 automated data.

2.2. Comprehensive digital image analysis of breast cancer immunohistochemical (ER, PR, HER2, Ki67) and CD8 biomarkers

2.2.1. Factor analysis of IHC, FISH, intratumoral heterogeneity and CD8+ cell density indicators

IHC, FISH, intratumoral heterogeneity, CD8+ cell density and imunogradient indicators were explored in the *HER2* non-amplified and amplified groups. The expression rates of ER and PR were higher, while Ki67 was lower in the *HER2* non-amplified group. The differences of intratumoral heterogeneity indicators were found only for Ki67 between two groups. Along with the higher *HER2* copy number, a significantly higher copy number of CEP17 was found in *HER2*-amplified tumors. No significant differences of CD8+ cell densities neither in tumor nor stroma areas nor inside the IZ (T, TE, and S aspects) between the groups were detected ($p > 0.05$). However, the mean of CD8+ density within the IZ was significantly higher in the S aspect than in the T aspect in both the *HER2* non-amplified and amplified ($p < 0.001$) groups. The variance of CD8+ cells was the highest in the S aspect, less in the TE aspect, and lowest in the T aspect of the IZ in *HER2* non-amplified group ($p < 0.0001$). The variation of CD8+ cell density was higher in the S aspect than in the T aspect of the IZ ($p < 0.0001$), while it was similar in the TE and S aspects of the IZ ($p > 0.05$) in *HER2*-amplified group; detailed summary statistics is published (43).

A factor analysis of combined set of DIA IHC, FISH, CD8+ cell density, and intratumoral heterogeneity data extracted 6 independent factors of variation in both analyzed groups (Figures 5 and 6).

In *HER2* non-amplified group, Factor 1 was represented by positive loadings of the variables indicative of CD8+ density within the IZ T, TE, and S aspects and was named CD8+ density factor. Factor 2 was characterized by positive loadings of HER2 FISH variables (*HER2* copy number, *HER2*/CEP17 ratio, percentage of amplified cells calculated from *HER2*/CEP17 ratio and by *HER2*

signals only) and was named the *HER2* amplification factor. Factor 3 was described by increasing CD8+ densities towards the T aspect of the IZ (strong positive loadings of the CD8 CM and its SD) and by moderate loading of CD8+ density in the T aspect; therefore, it was named the CD8+ density gradient. Factor 4 was represented by the Ki67% and Ki67 entropy indicators. Factor 5 was described by positive loadings of HER2 membrane completeness entropy and ER contrast, along with negative loading of ER%. This factor was interpreted as HER2&ER heterogeneity factor. Factor 6 was represented by PR% and PR entropy indicators.

Similarly, in HER2-amplified group, Factor 1 was the *HER2* amplification factor, Factor 2 was the CD8+ density factor, and Factor 3 (CD8+ density gradient factor) was the main sources of variance. Factor 4 was described by positive loadings of Ki67% and Ki67 entropy indicators and by negative loading of ER entropy. Factor 5 was represented by the percentage of both hormone receptors along with the PR entropy. Factor 6 was described by positive loading of a single HER2 membrane completeness variable.

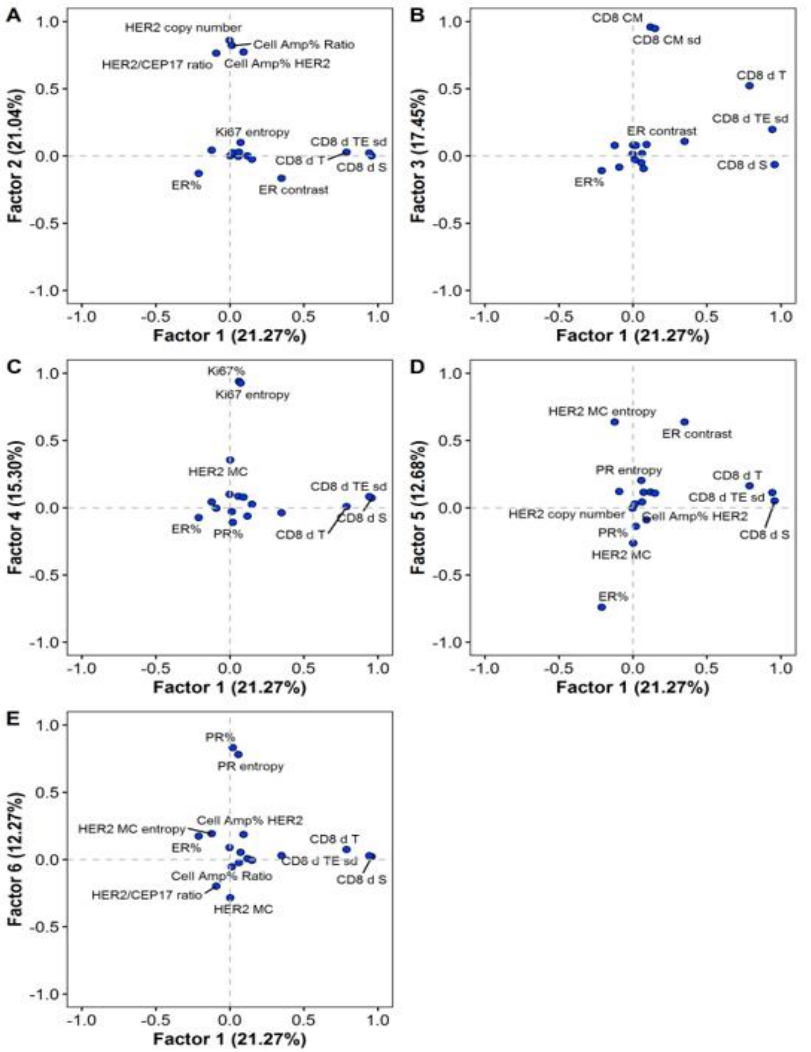

Figure 5. Rotated factor pattern in *HER2* non-amplified patients group: (A) the loadings of factors 1 and 2; (B) factors 1 and 3; (C) factors 1 and 4; (D) factors 1 and 5 and (E) factors 1 and 6 are plotted.

Cell_Amp_%_Ratio – percentage of amplified cells calculated from *HER2*/CEP17 ratio, Cell_Amp_%_*HER2* – percentage of amplified cells calculated by *HER2* signals only, CM – center of mass, CM_sd – standard deviation for center of mass, d_S – density in the stroma aspect of IZ, d_TE_sd – standard deviation in the tumor edge aspect of IZ, d_T – density in the tumor aspect of IZ, MC – membrane completeness.

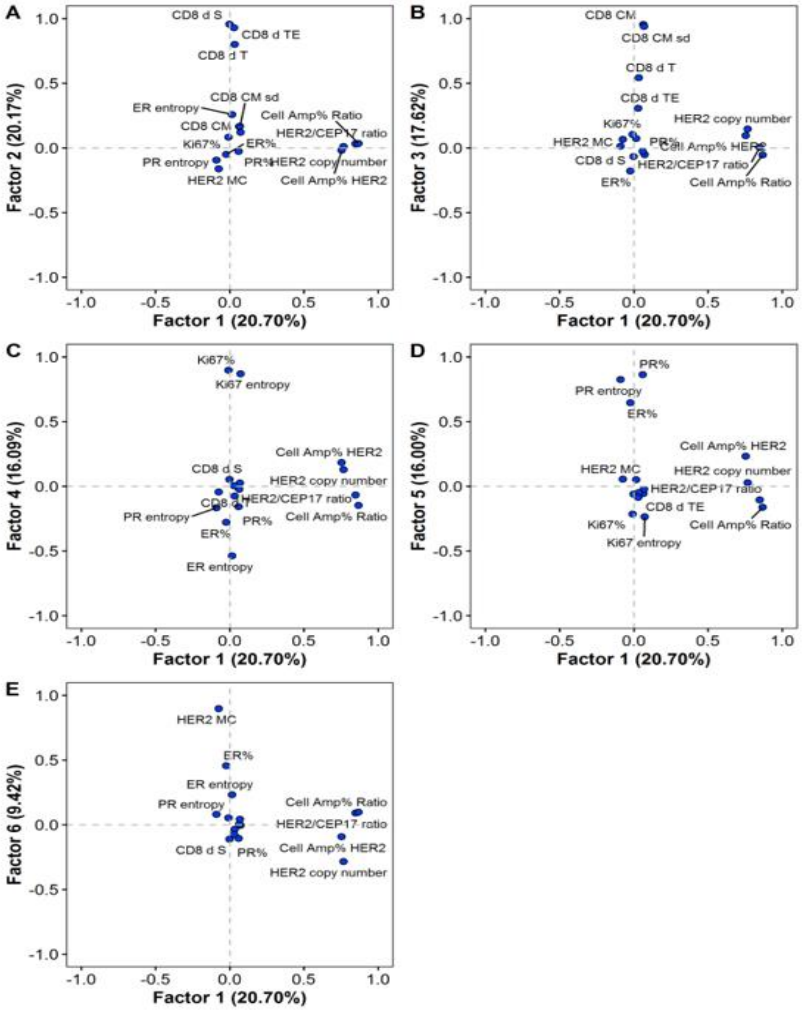

Figure 6. Rotated factor pattern in *HER2*-amplified patients group: (A) the loadings of factors 1 and 2, (B) factors 1 and 3, (C) factors 1 and 4, (D) factors 1 and 5 and (E) factors 1 and 6 are plotted.

Cell_Amp_%_Ratio – percentage of amplified cells calculated from *HER2*/CEP17 ratio, Cell_Amp_%_*HER2* – percentage of amplified cells calculated by HER2 signals only, CM – center of mass, CM_sd – standard deviation for center of mass, d_S – density in the stroma aspect of IZ, d_TE – density in the tumor edge aspect of IZ, d_T – density in the tumor aspect of IZ, MC – membrane completeness.

2.2.2. Prognostic value of IHC, FISH, intratumoral heterogeneity, CD8+ cell density indicators and clinicopathological indicators

The potential of the clinicopathological parameters, IHC, FISH, CD8+ cell density, and intratumoral heterogeneity indicators to predict OS of the patients was explored by univariate survival analysis. Statistically significant indicators are presented in Table 3.

Table 3. Univariate analysis of the impact of clinicopathological parameters, IHC, FISH, CD8+ cell density and intratumoral heterogeneity indicators in *HER2* non-amplified and amplified patient groups on overall survival using the log-rank test.

Indicators	**HR**	95% CI	*p*-Value	Cutoff value
HER2 non-amplified group				
pT stage (pT1–2 vs. pT3-4)	4.41	1.30–14.97	0.0173	-
pN stage (pN0 vs. pN1–3)	3.2	1.30–7.86	0.0111	-
HER2 %	0.25	0.11–0.62	0.001	16.62
HER2 MC	0.12	0.05–0.32	<0.0001	23.19
HER2_contrast	0.22	0.09–0.52	0.0002	0.65
HER2_dissimilarity	0.21	0.08–0.55	0.0005	0.44
HER2_entropy	0.23	0.10–0.56	0.0004	2.92
HER2_energy	4.28	1.81–10.08	0.0003	0.17
HER2_homogeneity	2.95	1.26–6.90	0.009	0.72
HER2 MC_contrast	0.37	0.14–0.94	0.029	0.41
HER2 MC_dissimilarity	0.36	0.14–0.92	0.025	0.34
HER2 MC_entropy	031	0.13–0.72	0.004	2.31
HER2 MC_energy	3.25	1.36–7.79	0.005	0.32
HER2 MC_homogeneity	2.9	1.18–7.13	0.015	0.83
ER_contrast	0.21	0.05–0.91	0.021	1.34
CD8_T	0.37	0.16–0.87	0.017	3.25
CD8_CM	0.2	0.08–0.49	<0.0001	-1.46
CD8_CM_sd	0.36	0.15–0.84	0.013	-1.08
CD8_d_S	3.22	0.94–11.05	0.049	6.10
CD8_d_S_sd	2.65	1.08–6.51	0.027	5.45
CD8_d_TE_sd	2.81	1.21–6.54	0.012	5.54
CD8_d_T	0.3	0.13–0.71	0.003	2.97
CD8_d_T_sd	0.35	0.14–0.85	0.016	3.94

CD8_ID	3.49	1.51–8.06	0.002	1.49
HER2-amplified group				
pT stage (pT1–2 vs. pT3-4)	3.49	1.01–12.05	0.049	-
pN stage (pN0 vs. pN1–3)	3.2	1.31–7.83	0.011	-
CEP17 copy number	0.25	0.09–0.68	0.003	1.93
HER2_entropy	0.4	0.16–1.02	0.047	3.98
HER2 MC_contrast	0.32	0.12–0.85	0.016	0.44
HER2 MC_dissimilarity	0.35	0.14–0.88	0.019	0.39
HER2 MC_homogeneity	2.49	0.99–6.27	0.044	0.81
Ki67_entropy	2.39	0.99–5.77	0.044	3.18
PR_AshD	3.72	1.35–10.26	0.006	3.66
CD8_T	0.38	0.16–0.91	0.024	3.58
CD8_CM	0.41	0.17–0.99	0.041	-0.89
CD8_d_TE	0.37	0.15–0.89	0.021	4.22
CD8_d_T	0.34	0.13–0.89	0.021	2.80
CD8_d_T_sd	0.35	0.14–0.89	0,022	4.35
CD8_ID	3.05	1.24–7.48	0.01	1.23

AshD – Ashman's D; *HER2* – human epidermal growth factor receptor 2; CEP17 – centromere enumeration probe for chromosome 17; CI – confidence interval; CM – center of mass; CM_sd – standard deviation for center of mass; d – density; ID – immunodrop; d_S – density in the stroma aspect of IZ; d_S_sd – standard deviation in the stroma aspect of IZ; d_T – density in the tumor aspect of IZ; d_T_sd – standard deviation in the tumor aspect of IZ; d_TE – density in the tumor edge aspect of IZ; d_TE_sd – standard deviation in the tumor edge aspect of IZ; MC – membrane completeness; sd – standard deviation; T – tumor area.

All the variables significantly associated with outcome at a univariate analysis ($p < 0.05$) were assessed for their independent prognostic value in the multivariate Cox regression models.

Three types of the models in each group were generated from different variable sets: (1) models produced from the pathological, IHC, FISH and intratumoral heterogeneity indicators; (2) models produced from the pathological, CD8+ cell density and immunogradient indicators; (3) models produced from the indicators of models types 1 and 2 (Tables 4 and 5 for the *HER2* non-amplified and amplified groups, respectively).

In the *HER2* non-amplified group, 3 independent predictors of better OS were revealed in model 1: higher values of HER2 membrane

completeness, HER2 membrane completeness entropy, and ER contrast (p = 0.0007; p = 0.0341 and p = 0.0449, respectively) predicted longer patient survival, while higher tumor stage was associated with worse OS ($p \leq 0.0014$).). In model 2, 3 independent indicators were identified: longer OS was associated with higher absolute CD8+ density in the tumor aspect of IZ (CD8_d_T) and positive IZ density gradient towards the tumor (CD8_CM) (p = 0.0079 and p = 0.0014, respectively), and worse OS with higher variance of the CD8+ cell density along the TE of IZ (CD8_d_TE_sd) (p = 0.0002). Remarkably, all three indicators of the model 2 had an independent value in the model 3 and markedly strengthened its prognostic power (model likelihood ratio 56.1, $p < 0{,}0001$ achieved in model 3 compared with that of 27.1, $p < 0{,}0001$ in model 1).

In the *HER2*-amplified group, higher values of HER2 membrane completeness contrast and CEP17 copy number indicators (p = 0.0367 and p = 0.0035, respectively) predicted longer patient survival, while pN was associated with worse OS (p = 0.0018) (model 4). In model 5, higher CD8+ density in the tumor aspect of IZ was an independent factor of better OS (p = 0.0047) in the context of worse OS predicted by pN status (p = 0.0023). The prognostic power of the 6 model was increased by the adding CD8+ density and immunogradient indicators to the model 4 (likelihood ratio 29.03, $p < 0{,}0001$ of model 6 compared with 17.64, p = 0.0005 of model 4).

The Kaplan–Meier survival probability plots demonstrating an association between the independent prognostic factors and OS are presented for the *HER2* non-amplified and amplified groups in Figures 7, 8, respectively.

Table 4. Multivariate analysis of prognostic factors associated with OS in *HER2* non-amplified group.

Indicator	HR	95% CI	*p*-Value
Model 1 (LR: 27.1, $p < 0.0001$)			
pT stage (pT1–2 vs. pT3-4)	6.04	2.31–33.04	0.0014
HER2 MC	0.18	0.07–0.48	0.0007
HER2 MC_entropy	0.37	0.15–0.93	0.0341
ER_contrast	0.21	0.05–0.97	0.0449
Model 2 (LR: 28.26, $p < 0.0001$)			
CD8_CM	0.14	0.04–0.47	0.0014
CD8_d_T	0.23	0.08–0.68	0.0079
CD8_d_TE_sd	9.45	2.9–30.78	0.0002
Model 3 (LR: 56.05, $p < 0.0001$)			
pT stage (pT1–2 vs. pT3-4)	13.65	3.05–61.03	0.0006
HER2 MC	0.17	0.05–0.66	0.0102
HER2 MC_entropy	0.33	0.13–0.88	0.0263
ER_contrast	0.16	0.03–0.80	0.0258
CD8_CM	0.223	0.08–0.64	0.0053
CD8_d_T	0.147	0.05–0.47	0.0013
CD8_d_TE_sd	7.82	2.63–23.28	0.0002

HER2 – human epidermal growth factor receptor 2; CI – confidence interval; CM – center of mass; d_T –density in the tumor aspect of IZ; d_TE_sd – standard deviation in the tumor edge aspect of IZ; HR – hazard ratio; LR – likelihood ratio; MC – membrane completeness; OS – overall survival.

Table 5. Multivariate analysis of prognostic factors associated with OS in *HER2*-amplified group.

Indicator	HR	95% CI	*p*-Value
Model 4 (LR: 17.64, $p = 0.0005$)			
pN stage (pN0 vs. pN1–3)	4.75	1.77–12.62	0.0018
HER2 MC_contrast	0.35	0.13–0.94	0.0367
CEP17 copy number	0.191	0.06–0.58	0.0035
Model 5 (LR: 12.52, $p = 0.0019$)			
pN stage (pN0 vs. pN1–3)	4.55	1.72–12.06	0.0023
CD8_d_T	0.22	0.08–0.63	0.0047
Model 6 (LR: 29.03, $p < 0.0001$)			
pN stage (pN0 vs. pN1–3)	7.985	2.7–23.63	0.0002
HER2 MC_contrast	0.243	0.09–0.69	0.0077
CEP17 copy number	0.135	0.04–0.44	0.0008
CD8_d_T	0.117	0.04–0.37	0.0002

HER2 – human epidermal growth factor receptor 2; CEP17 – centromere enumeration probe for chromosome 17; CI – confidence interval; d_T –density in the tumor aspect of IZ; HR – hazard ratio; LR – likelihood ratio; MC – membrane completeness; OS – overall survival.

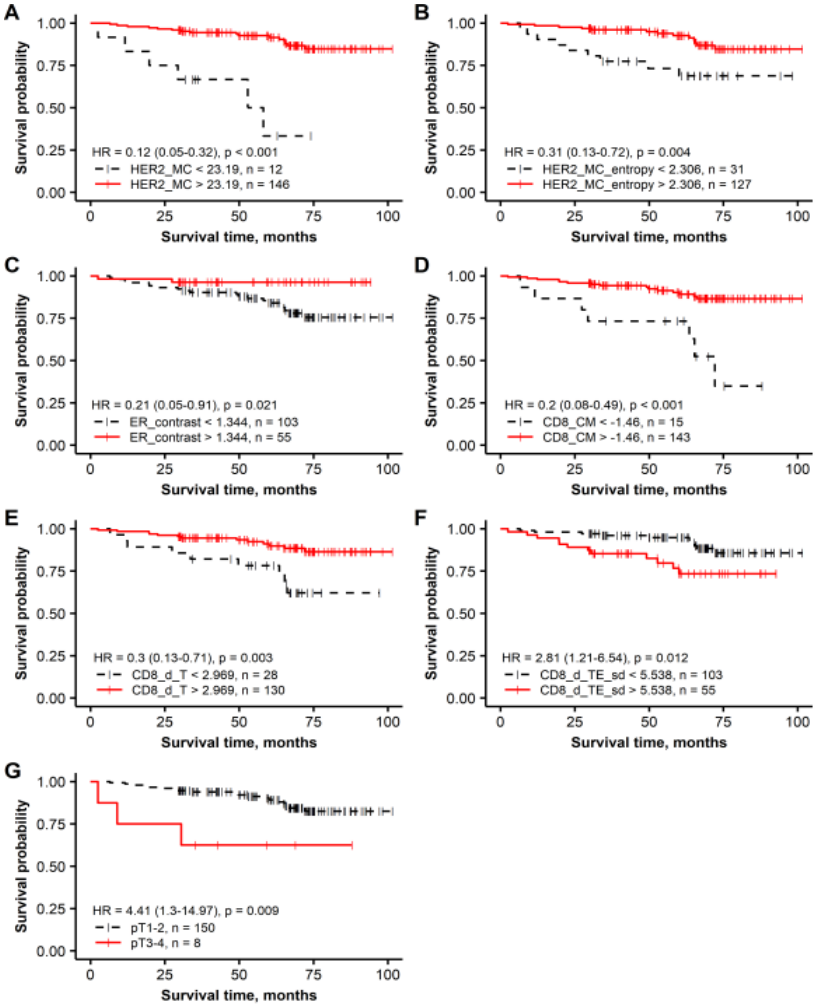

Figure 7. Kaplan–Meier survival plots representing the association of overall survival in the group of patients with *HER2* non-amplified breast cancer with independent prognostic indicators identified by multiple Cox regression analysis: (A) membrane completeness (HER2 MC), (B) membrane completeness entropy (HER2 MC entropy), (C) ER contrast, (D) center of mass for CD8+ density (CD8_CM), (E) mean CD8+ density in the tumor aspect (CD8_d_T), (F) standard deviation of CD8+ density in the tumor edge aspect (CD8_d_TE_sd), and (G) tumor stage (T).

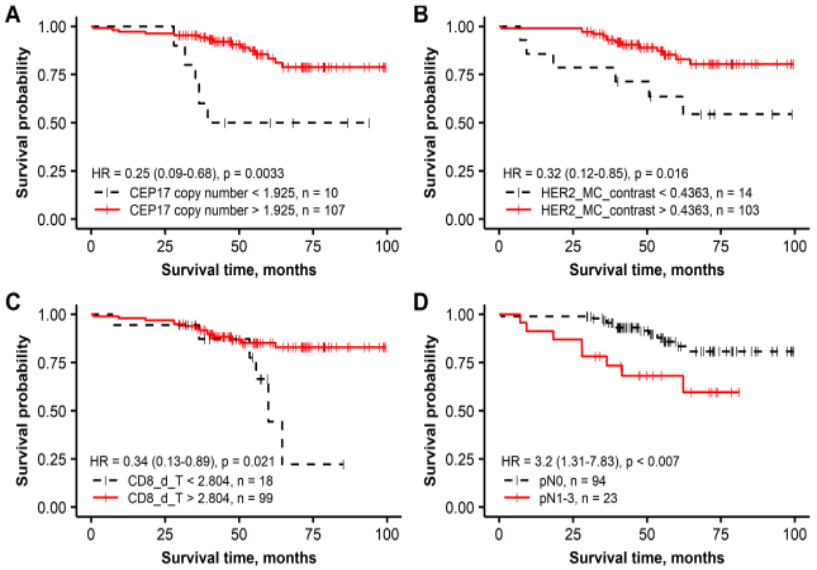

Figure 8. Kaplan–Meier survival plots representing the association of overall survival in the group of patients with *HER2*-amplified breast cancer with independent prognostic indicators identified by multiple Cox regression analysis: (A) CEP17 copy number, (B) membrane completeness contrast (HER2 MC contrast), (C) mean CD8+ density in the tumor aspect (CD8_d_T), and (D) lymph node status (pN).

DISCUSSION

We investigated the possibility to evaluate *HER2* gene status in breast cancer tissue by automated FISH image analysis (StrataQuest v.205 program (TissueGnostics, Austria)). Significantly lower mean copy numbers of *HER2* and CEP17 and mean *HER2*/CEP17 ratio were counted by the automated procedure compared to the manual procedure data in the analysis of 50 IHC borderline (2+) cases of invasive ductal breast carcinoma. Therefore, image analysis can not readily be used as clinical decision support tool to measure the level of *HER2* amplification. This is due to potential differences in cell selection criteria in both techniques: while FISH signals are counted manually in a limited number of “more suspicious" cells with more abundant *HER2* signals, the image analysis takes into account all segmented nuclei of cancer cells.

However, high-capacity nonselective tumor cell assay enables unbiased, continous data to represent large cell populations and indicate potential intratumoral heterogeneity with regard to *HER2* status. Statistical indicators of bimodality were linearly independent of the level of *HER2* amplification or increased CEP17 copy number (or *HER2*/CEP17 ratio) in our study. This suggests that objective and quantifiable measurement of intratumoral heterogeneity can be achieved. The concept of genetical heterogeneity is largely based only on a fraction of the amplified cells (22, 25) and as demonstrated by Chang et al. (23), depends on the overall level of amplification. Meanwhile, the bimodality indicators reflect specifically the distribution pattern of the cell population tested. In addition, based on the extracted of linearly independent scores of amplification, polysomy, and bimodality, the stratification of cases into relatively homogenous (unimodal) and heterogenous (bimodal) tumors, is possible. The latter category only partially overlapped to the conventional genetically heterogeneous cases. We therefore conclude that an automated high-capacity nonselective tumor cell assay can

generate evidence-based *HER2* intratumor heterogeneity indicators to refine definitions of genetical heterogeneity.

We investigated the prognostic significance of IHC, FISH, intratumoral heterogeneity, CD8+ cell density and clinical and pathological parameters in HER2 IHC 2+ FISH-negative and FISH-positive patients using hexagonal tiling analytics of DIA data and established prognostic models of OS, which take into account spatial aspects of intratumoral heterogeneity and tumor immune microenvironment.

Only two IHC variables – HER2 expression percentage and HER2 membrane completeness were found as significantly associated with the patient outcome (HR = 0.25, $p = 0.001$ and HR = 0.12, $p < 0.0001$, respectively (data not shown)) in the *HER2* non-amplified group. Of these, HER2 membrane completeness was a stronger indicator than the proportion of HER2-positive tumor cells and, together with two intratumoral heterogeneity indicators – HER2 membrane completeness entropy and ER contrast were identified as independent predictors of good prognosis associated with longer OS in multivariate Cox regression models (table 4, models 1 and 3). Similarly to our findings, the association of higher HER2 expression with better patient prognosis was found in a univariate analysis in a recent study of early hormone receptor-positive breast cancer patients (44).

The associations of ER contrast with HER2 membrane completeness entropy and their inverse relation to ER expression were revealed by factor analysis (Factor 5, Figure 5). This HER2&ER heterogeneity factor reflects the higher intratumoral heterogeneity of both HER2 and ER proteins in the tumors with decreased ER expression. Of note, ER contrast was the only intratumoral heterogeneity indicator of hormone receptors that provided the independent prognostic value (Table 4, HR = 0.21, $p = 0.0449$, model 1, HR = 0.16, $p = 0.0258$, model 3, respectively). In addition, ER intratumoral heterogeneity indicator showed a greater prognostic value than the rate of its expression. The findings that the intratumoral

heterogeneity indicators of Ki67 and PR expression enabled higher prognostic power than the expression rates *per se* has been demonstrated in previous studies (38, 40, 44).

The prognostic models obtained in *HER2*-amplified group should be taken with caution, as the OS of these patients is likely to have been impacted by the targeted therapy, which was applied to the majority of patients in this subgroup (87, 74.4%). In multiple Cox regression models, a greater prognostic value of intratumoral heterogeneity of HER2 expression indicator (membrane completeness contrast) than the rate of its expression (membrane completeness) was founded (Table 5, HR = 0.35, $p = 0.0367$, Model 4 and HR = 0.243, $p = 0.0077$, Model 6). The association of another independent prognostic factor, CEP17, with longer patient survival is unclear, as it may be related to various treatment modalities applied in *HER2*-amplified breast cancer patients.

Our study demonstrated that the assessement of CD8+ cell density variation in the automatically extracted tumor-stroma IZ is more informative than the conventional measurements of TIL density in the tumor microenvironment. The higher CD8+ cell densities in the tumor compartment were associated with longer OS in univariate analyses in both patient subgroups (HR = 0.37, $p = 0.017$ and HR = 0.38, $p = 0.024$ in the *HER2* non-amplified and amplified groups, respectively (data not shown)), however, they did not provide the independent prognostic value in multivarite Cox regression models. In contrast, three indicators extracted from the tumor-stroma IZ provided the independent prognostic value in the *HER2* non-amplified tumors: CD8+ density in the tumor aspect of IZ and positive IZ CD8+ density gradient towards the tumor were associated with longer OS, while the standard deviation of CD8+ density along the TE predicted worse OS. Importantly, prediction of OS for patients was possible based exclusively on these 3 indicators computed from DIA data obtained from a single CD8 IHC slide per patient (Table 4, model 2). Moreover, supplementing the model with CD8+ cell density and immunogradient indicators markedly increased the power of the prognostic model

(Table 4, model 3). Similar results were presented by Rasmusson et al. (34), where both CD8+ density in the tumor aspect of IZ and CM for CD8+ cell density within the IZ indicators were independent predictors of a longer OS in early hormone receptor-positive breast cancer. The results of the prognostic value of CD8+ lymphocytes in patients with hormone receptor-positive/HER2-negative tumors are conflicting: while a favorable prognosis for higher CD8+ cell density in node-negative breast cancer (45), as well as in a combined analysis with CD163+ (46) has been reported, other studies have shown an increased level of CD8+ lymphocytes associated with poor prognosis (35, 47, 48) or reported no statistically significant association between CD8+ cells and patient prognosis (49).

In the *HER2*-amplified group, CD8+ cell density in the tumor aspect of the IZ was the only idependent prognostic factor associated with longer OS. Reportedly, an abundant TIL infiltration has been associated with better outcomes (pathological complete response, event-free survival, and disease-free survival) in HER2-positive breast cancer (50-52), but the prognostic significance of CD8+ TILs still remains controversial (35, 48, 49, 53, 54). These conflicting results confirm the need for methods with appropriate discriminatory spatial precision to assess the spatial aspects of the distribution of TILs and expose their prognostic role in different breast cancer subtypes.

In summary, we present novel prognostic models based on computational intratumoral heterogeneity and immune response (generated from CD8+ cell density measurements) indicators of the IHC biomarkers in HER2 IHC 2+ borderline breast cancer patients.

In this study, we also explored the local intratumoral associations between PR and HER2 expression by applying double IHC staining for PR and HER2 with DIA and subsequent hexagonal grid analytics (data not published). The detected significant local associations of both biomarkers could reflect local tumor progression in HER2 borderline and heterogeneous cases and provide potential practical benefits in tissue sampling for *HER2* FISH testing. Further studies are

needed to investigate biological and clinical aspects of local hormone receptors and HER2 interactions in the tumor microenvironment.

CONCLUSIONS

1. Significantly lower values of *HER2* amplification were obtained by the automated *HER2* FISH image analysis, compared to the manual procedure. Therefore, automated evaluation of *HER2* gene status by FISH using the digital image analysis algorithms used in our study cannot be directly applied for the quantitative evaluation of *HER2* amplification due to the systematic bias compared to conventional microscopy methods according to the current clinical guidelines. The bias is, most likely, caused by differences in cell selection criteria for the manual and automated procedures.
2. Digital *HER2* FISH image analysis of large tumor cell populations provides new opportunities to assess intratumoral *HER2* gene heterogeneity. The calculated bimodality indicators for *HER2*, CEP17, and their ratio are linearly independent of *HER2* amplification and increased CEP17 copy number, and enable quantitative assessment of their intratumoral heterogeneity.
3. Intratumoral heterogeneity indicators of HER2 and ER IHC expression detected using hexagonal tiling analytics of digital image analysis outputs are independent prognostic factors of overall survival in HER2 IHC 2+ bordeline breast cancer patients. HER2 membrane completeness entropy and ER contrast in the *HER2* non-amplified group and HER2 membrane completeness contrast in the *HER2*-amplified group are independent prognostic factors of longer overall survival.
4. Computational indicators of CD8+ lymphocyte distribution in the tumor microenvironment, obtained by the interface zone immunogradient method, provided independent prognostic value. In the *HER2* non-amplified group, 3 independent indicators (CD8+ cell density in the tumor aspect, CD8+ center of mass, standard deviation for CD8+ density in the tumor edge aspect), generated from single CD8 IHC DIA data, predicted overall

patient survival without requirement for any other variables available in this study. In the *HER2*-amplified group, the CD8+ cell density in the tumor aspect of the interface zone was the only antitumor immune response feature with independent contribution to the overall survival prognostic model.

PUBLICATIONS AND PRESENTATIONS

Publications:

1. **Radziuviene G**, Rasmusson A, Augulis R, Lesciute-Krilaviciene D, Laurinaviciene A, Clim E, Laurinavicius A: Automated Image Analysis of HER2 Fluorescence In Situ Hybridization to Refine Definitions of Genetic Heterogeneity in Breast Cancer Tissue. *BioMed Research International*, 2017; 2017:2321916.
2. **Radziuviene G**, Rasmusson A, Augulis R, Grineviciute R. B, Zilenaite, D, Laurinaviciene A, Ostapenko V, Laurinavicius A: Intratumoral heterogeneity and immune response indicators to predict overall survival in HER2-bordeline (IHC2+) breast cancer patients. *Front Oncol.*, 2021; 11:774088.

Presentations:

1. **Radziuviene G.** Digital image analysis for Human epidermal growth factor receptor 2 (HER2). 2nd International scientific and practical conference „Molecular techniques in tissue-based pathology diagnosis“, 2014. Vilnius, Lithuania.
2. **Radziuviene G,** Rasmusson A, Augulis R, Lesciutė-Krilaviciene D, Laurinaviciene A, Clim E, Laurinavicius A: Automated Image Analysis of HER2 FISH Enables New Definitions of Genetic Heterogeneity in Breast Cancer Tissue. 13th European Congress on Digital Pathology, 2016. Berlin, Germany.

Poster presentations:

1. **Radziuviene G**, Rasmusson A, Augulis R, Lesciute-Krilaviciene D, Laurinaviciene A, Clim E, Laurinavicius A: Automated Image Analysis of *HER2* FISH in Breast Cancer Tissue to Support Cell Heterogeneity, 3rd Nordic Symposium on Digital Pathology, 2015. Linkoping, Sweden.

2. **Radziuviene G**, Rasmusson A, Augulis R, Grineviciute R. B, Zilenaite, D, Laurinaviciene A, Ostapenko V, Laurinavicius A: Intratumoral heterogeneity and immune response indicators to predict overall survival in HER2-bordeline (IHC2+) breast cancer patients., *Life Sciences Baltics* 2021. Vilnius, Lithuania.

SUMMARY IN LITHUANIAN

Darbo aktualumas

Krūties vėžys yra viena dažniausių moterų onkologinių ligų (1, 2). Pastaraisiais dešimtmečiais atsiradę naujesni ir modernesni gydymo būdai – taikinių terapija, imunoterapija, atveria galimybę gerinti pacienčių gydymą. Krūties vėžys yra sudėtinga ir įvairialypė liga, kuriai būdingos skirtingos klinikinės, patologinės ir molekulinės savybės. Daugialypis jos pobūdis lemia įvairias klinikines baigtis ir skirtingus terapinius atsakus. Kasdienėje klinikinėje praktikoje krūties vėžio prognozės nustatymas ir gydymo parinkimas jau daugelį metų remiasi klinikiniais ir patologiniais parametrais – naviko stadija (T), sritinių limfmazgių būkle (N), histologiniu diferenciacijos laipsniu (G) ir biožymenų – estrogenų receptorių (ER), progesterono receptorių (PR) raiška, žmogaus epidermio augimo veiksnio receptoriaus 2 (HER2, angl. *the human epidermal growth factor receptor 2*) būkle (4). Tačiau, siekiant parinkti tinkamą ir veiksmingą individualų gydymą pacientui, šių kriterijų nepakanka (5). Todėl aktyviai ieškoma naujų prognozinių krūties vėžio biožymenų ir jie tyrinėjami (6).

Apie 15–20 % invazinio krūties vėžio atvejų sukelia *HER2* onkogeno amplifikacija ir (arba) padidėjusi baltymo raiška (7, 8). Tai itin agresyvi ir blogos prognozės liga, todėl patikimų biologinių žymenų, kurie pagerintų pacientų atranką esamoms ir būsimoms metastazavusio krūties vėžio gydymo strategijoms (9), taip pat prognozuotų ligos atkrytį (11) bei atsparumą anti-HER2 terapijai (10), poreikis yra ypač aktualus. HER2 yra ne tik prognozinis žymuo, bet ir svarbus biologinės terapijos taikinys – jau daugiau kaip prieš du dešimtmečius HER2 teigiamo krūties vėžio gydymui taikomas monokloninis antikūnas trastuzumabas (*Herceptin; Genentech, South San Francisco*, JAV) stabdo ligos progresavimą ir gerokai pailgina pacientų išgyvenamumą (12-14). Todėl tikslus HER2 būklės įvertinimas, siekiant taikyti efektyvią individualizuotą terapiją, yra labai svarbus.

Tačiau net po kelis dešimtmečius trukusių plačių krūties vėžio HER2 būklės tyrimų standartizuotomis metodikomis ir klinikiniais testų rezultatais pagrįstos pacientų atrankos HER2 taikininei terapijai, HER2 diagnostikoje yra likę svarbių neatsakytų klausimų. Dauguma HER2 teigiamų ir neigiamų atvejų yra lengvai įvertinami *ASCO/CAP* (angl. *American Society of Clinical Oncology/College of American Pathologists*) gairėse rekomenduojamais imunohistochemijos (IHC), kuriuo nustatoma baltymo raiška ir *in situ* hibridizacijos, kuriuo nustatoma geno amplifikacija, metodais (15), tačiau paribinių atvejų inerpretacija yra sudėtingesnė. Pastarieji atvejai dažnai yra heterogeniški, juose būna padidėjęs 17 chromosomos centromeros kopijų (CEP17) skaičius, o tai sąlygoja tyrėjų atliekamo vertinimo neatitikimus ir, svarbiausia, kelia terapijos taikymo dilemą (16-20). Paribinių atvejų, sudarančių apie 18 % krūties vėžio atvejų, interpretacijos sunkumus atspindi vis besikeičiantys rekomenduojami jų vertinimo kriterijai (15, 21, 22).

Itin aktuali yra HER2 amplifikacijos bei raiškos naviko audinyje heterogeniškumo vertinimo problema. Heterogeniškų navikų IHC ir fluorescencinės *in situ* hibridizacijos (FISH) tyrimų rezultatai yra prieštaringi, nulemiantys netikslią HER2 būklės interpretaciją bei netinkamą gydymo parinkimą ir atsaką į jį (16, 23, 24). Gairėse nurodytas *HER2* genetinio heterogeniškumo apibrėžimas (25) sulaukė nemažai diskusijų, kritikos ir siūlymų jį modifikuoti (23, 26-28). Dabartinis genetinio heterogeniškumo vertinimo būdas, kuris remiasi vizualia riboto ląstelių skaičiaus analize, nesuteikia informacijos apie tikrąją *HER2* raiškos variaciją. Gairėse taip pat nėra pateikta HER2 IHC raiškos heterogeniškumo vertinimo rekomendacijų. Pusiau kiekybinis HER2 IHC tyrimo metodas riboja galimybę išmatuoti atskirų naviko ląstelių ar sričių įvairovę, nors viena verte įvertinti navikai gali būti sudaryti iš heterogeniškų sričių. Dėl šių priežasčių yra labai reikalingas objektyvus ir patikimas heterogeniškumo reiškinio vertinimo tiek baltymo, tiek geno lygmeniu metodas. Heterogeniškumas riboja terapijų efektyvumą, todėl svarbu įvertinti ne tik HER2, bet ir hormonų receptorių raiškos įvairovę.

Dar vienas reikšmingas HER2 būklės tyrimo variacijos šaltinis yra CEP17 kopijų skaičiaus pokyčiai (padidėjimas arba sumažėjimas) (19, 29). Jie gali nulemti klaidingus analizės rezultatus, ypač paribiniais atvejais, todėl tikslus ir objektyvus CEP17 kopijų skaičiaus variacijos įvetinimas taip pat yra būtinas.

Pastarųjų metų intensyvūs naviko mikroaplinkos tyrimai atskleidė prognozinę imuninio atsako svarbą sergant krūties vėžiu (30, 31). Vieni iš pagrindinių jos komponentų – naviką infiltruojantys limfocitai – yra siejami su geresne prognoze – didesnis jų kiekis lemia stipresnį imuninį atsaką į vėžines ląsteles ir paskirtą gydymą, tačiau skirtingų krūties vėžio potipių duomenys yra prieštaringi (32, 33). Siekiant atrasti reikšmingą papildomą naviką infiltruojančių limfocitų prognozinę informaciją pacienčių, kurioms nustatyta paribinė HER2 baltymo raiška, grupėje, reikalingi išsamesni, ne tik naviką infiltruojančių limfocitų tankio, bet ir jų erdvinio pasiskirstymo navikiniame audinyje tyrimai moderniais, skaitmenine vaizdo analize pagrįstais metodais.

Darbo tikslas

Skaitmeninės vaizdo analizės metodais nustatyti *HER2* onkogeno amplifikacijos ir raiškos variacijos šaltinius ir ištirti prognozinius rodiklius pacienčių, sergančių krūties vėžiu, kai nustatyta HER2 paribinė baltymo raiška, imtyje.

Darbo uždaviniai

1. Automatizuoti *HER2* geno būklės vertinimą FISH metodu, pritaikant skaitmeninės vaizdo analizės algoritmus, ir palyginti tyrėjų vertinimus su automatizuotais *HER2* amplifikacijos matavimais.
2. Naudojantis FISH skaitmeninės vaizdo analizės duomenimis nustatyti *HER2* kopijų skaičiaus variaciją navikiniame audinyje ir

įvertinti šio heterogeniškumo ir padidėjusio CEP17 kopijų skaičiaus įtaką *HER2* FISH testo rezultatams.
3. Skaitmeninės vaizdo analizės metodais išmatuoti HER2, ER, PR ir Ki67 žymenų raiškos heterogeniškumą krūties vėžio audinyje ir nustatyti jo prognozinę vertę esant paribinei HER2 raiškai.
4. Įvertinti CD8+ limfocitų pasiskirstymo krūties vėžio mikroaplinkoje rodiklius ir jų prognozinę vertę kitų prognozinių krūties vėžio požymių kontekste.

Ginamieji teiginiai

1. Skaitmeninė didelės apimties *HER2* FISH vaizdo analizė atveria naujas galimybes kiekybiškai įvertinti *HER2* geno raiškos heterogeniškumą krūties vėžio audinyje.
2. IHC biožymenų vidunavikinio heterogeniškumo rodikliai krūties vėžio audinyje leidžia prognozuoti pacienčių, sergančių krūties vėžiu, kurioms nustatyta paribinė HER2 baltymo raiška, bendrąjį išgyvenamumą.
3. Krūties vėžio audinyje naviko ir stromos sąveikos zonoje nustatyti CD8+ ląstelių tankio rodikliai yra nepriklausomi prognoziniai pacienčių, sergančių krūties vėžiu, kurioms nustatyta paribinė HER2 baltymo raiška, bendrojo išgyvenamumo veiksniai.

Darbo naujumas

Šiame darbe taikyti skaitmeninės mikroskopinių vaizdų analizės metodai padėjo atskleisti HER2 amplifikacijos ir raiškos ypatumus, leidžiančius optimizuoti krūties vėžio diagnostikos metodus ir nustatyti reikšmingus prognozinius veiksnius pacienčių, sergančių krūties vėžiu, kurioms diagnozuota HER2 baltymo paribinė raiška (IHC 2+), imtyje.

Pirmą kartą *HER2* geno raiškos vidunavikiniam heterogeniškumui įvertinti pritaikyti automatizuoti FISH analizės algoritmai. Darbe pristatyti nauji kiekybiniai heterogeniškumo (bimodalumo) matavimo

rodikliai, įvertinantys *HER2* signalų variaciją krūties vėžio ląstelėse. Ši matematiniu būdu gaunama informacija apie *HER2* vidunavikinį heterogeniškumą gali papildyti dabartinę *HER2* genetinio heterogeniškumo koncepciją, kuri remiasi riboto ląstelių skaičiaus vertinimu ir yra priklausoma nuo amplifikacijos laipsnio.

Taikydami skaitmeninę vaizdo analizę kartu su šešiakampių gardelių metodika kiekybiškai išmatavome HER2 baltymo ir kitų standartinių krūties vėžio IHC biožymenų – ER, PR ir Ki67 – raiškos heterogeniškumą navikiniame audinyje. Iki šiol išsami šių žymenų heterogeniškumo analizė esant paribinei HER2 raiškai nebuvo atlikta. Nustatyti nepriklausomi prognoziniai HER2 ir ER biožymenų vidunavikinio heterogeniškumo rodikliai, kurie papildo krūties vėžio klinikos ir patologijos parametrus ir pranoksta kitus kiekybinius IHC žymenų vertinimo rodiklius.

Šiame tyrime įvertinome vieną pagrindinių imuninio atsako komponentų – CD8+ limfocitų prognozinę reikšmę krūties navikuose, kai nustatyta paribinė HER2 baltymo raiška. Ankstesnių tyrimų duomenys vertinant CD8+ prognozinę reikšmę ir *HER2* neamplifikuotuose (hormonų receptoriams teigiamuose), ir amplifikuotuose navikuose yra prieštaringi (33, 35). Nustatėme naujus nepriklausomus prognozinius bendrojo išgyvenamumo veiksnius, paremtus CD8+ limfocitų pasiskirstymo krūties vėžio mikroaplinkoje rodikliais: *HER2* amplifikuotoje grupėje CD8+ ląstelių tankį naviko srityje, *HER2* neamplifikuotoje grupėje – CD8+ ląstelių tankį naviko srityje, CD8+ ląstelių tankio gradientą į naviką ir CD8+ ląstelių tankio standartinį nuokrypį naviko krašte. Pastarojoje grupėje šie trys rodikliai (ir jų derinys) leido nepriklausomai nuo kitų klinikos ir patologijos parametrų prognozuoti pacienčių bendrąjį išgyvenamumą.

Mūsų taikyti analizės metodai atskleidė naujus hormonų receptorių ir HER2 raiškos sąveikos naviko mikroaplinkos regioniniu lygmeniu. Dvigubas PR ir HER2 žymenų IHC dažymas, jų skaitmeninė vaizdo analizė ir šešiakampių gardelių analitika leido įvertinti lokalias PR ir HER2 biožymenų raiškos sąsajas. Nustatytas lokalios transformacijos iš PR vyraujančios raiškos ląstelėse į HER2 dominuojančias ląstelių

populiacijas reiškinys, yra susijęs su lokaliai padidėjusiu navikinių ląstelių tankiu. Manome, kad šis reiškinys gali būti specifinis krūties vėžio progresijos požymis, paaiškinantis paribinės ir erdviškai heterogeniškos HER2 raiškos veiksnius hormonų receptoriams teigiamuose navikuose. Lokalios transformacijos reiškinys gali turėti ir praktinės reikšmės, tikslingai atrenkant mėginius FISH tyrimams. Šie radiniai reikalauja tolesnių tyrimų.

IŠVADOS

1. *HER2* geno būklės tyrimas FISH metodu, taikant automatizuotos skaitmeninės vaizdo analizės algoritmus, aptinka sistemiškai mažesnes *HER2* amplifikacijos vertes, palyginti su įprastiniu mikroskopijos metodu, paremtu labiau amplifikuotų ląstelių atranka vertinimui. Todėl neatrankus skaitmeninis kiekybinis amplifikacijos vertinimas negali būti tiesiogiai taikomas klinikinėje praktikoje.
2. Didelės apimties skaitmeninė *HER2* FISH vaizdų analizė suteikia naujas galimybes vertinti vidunavikinį *HER2* geno raiškos heterogeniškumą. Apskaičiuoti *HER2*, CEP17 ir jų santykio bimodališkumo rodikliai linijiniu požiūriu nepriklauso nuo amplifikacijos laipsnio ir padidėjusio CEP17 kopijų skaičiaus ir leidžia kiekybiškai įvertinti jų variaciją navikiniame audinyje.
3. Skaitmeninės vaizdo analizės ir šešiakampių gardelių analitikos metodais nustatyti HER2 ir ER žymenų raiškos vidunavikinio heterogeniškumo rodikliai yra nepriklausomi prognoziniai bendrojo išgyvenamumo veiksniai pacienčių, sergančių krūties vėžiu, kai yra nustatyta HER2 baltymo paribinė raiška, imtyje. *HER2* neamplifikuotoje grupėje HER2 membranos vientisumo entropija ir ER kontrastas, o *HER2* amplifikuotoje grupėje - HER2 membranos vientisumo kontrastas yra nepriklausomi ilgesnio pacienčių bendrojo išgyvenamumo prognoziniai veiksniai.
4. Pacienčių, kurioms nustatyta paribinė HER2 baltymo raiška, imtyje, nustatyta CD8+ limfocitų pasiskirstymo krūties vėžio mikroaplinkoje rodiklių nepriklausoma prognozinė vertė. *HER2* neamplifikuotų navikų grupėje trys apskaičiuotieji imuninio atsako rodikliai, pagrįsti CD8+ žymens matavimais naviko ir stromos sąveikos zonoje (CD8+ ląstelių tankis naviko srityje, CD8+ ląstelių tankio gradientas į naviką ir CD8+ ląstelių tankio standartinis nuokrypis naviko krašte) leidžia patikimai ir nepriklausomai nuo kitų klinikos ir patologijos parametrų

prognozuoti pacienčių bendrąjį išgyvenamumą. *HER2* amplifikuotų navikų grupėje CD8+ ląstelių tankis sąveikos zonos naviko srityje yra vienintelis nepriklausomas prognozinis antinavikinio imuninio atsako rodiklis.

CURRICULUM VITAE

Name, surname	Gedmantė Radžiuvienė
Date of birth	September 9, 1976
Contact information	Phone: +370 65369440
	E-mail: gedmante.radziuviene@vpc.lt

EDUCATION

2012–2021	Vilnius University, Life Sciences Center, Institute of Biosciences. Doctoral studies in Biomedical Sciences
1998–2000	Vilnius University, Faculty of Natural Sciences. Master's degree in Genetics
1994–1998	Vilnius University, Faculty of Natural Sciences. Bachelor's degree in Molecular Biology

WORK EXPERIENCE

2007–present	Medical geneticist at the National Center of Pathology, Affiliate of Vilnius University Hospital Santaros Klinikos, Vilnius, Lithuania
2006–2007	Analyst, „Sicor Biotech" („Teva Baltic"), Production site, Vilnius, Lithuania
2000–2006	Researcher, „Sicor Biotech" („Teva Baltic"), Research&Development subdivision, Vilnius, Lithuania

REFERENCES

1. Prieiga internete: https://www.nvi.lt/vezio-registras/.
2. Sung H, Ferlay J, Siegel RL, Laversanne M, Soerjomataram I, Jemal A, et al. Global Cancer Statistics 2020: GLOBOCAN Estimates of Incidence and Mortality Worldwide for 36 Cancers in 185 Countries. CA Cancer J Clin. 2021;71(3):209-49.
3. Daiva G, Laura S, Nadežda L. Krūties vėžys Lietuvoje. Acta medica Lituanica. 2015;22(3).
4. Cardoso F, Kyriakides S, Ohno S, Penault-Llorca F, Poortmans P, Rubio IT, et al. Early breast cancer: ESMO Clinical Practice Guidelines for diagnosis, treatment and follow-up. Ann Oncol. 2019;30(10):1674.
5. Rakha EA, Pareja FG. New Advances in Molecular Breast Cancer Pathology. Semin Cancer Biol. 2021;72:102-13.
6. Wu HJ, Chu PY. Recent Discoveries of Macromolecule- and Cell-Based Biomarkers and Therapeutic Implications in Breast Cancer. Int J Mol Sci. 2021;22(2).
7. Slamon DJ, Clark GM, Wong SG, Levin WJ, Ullrich A, McGuire WL. Human breast cancer: correlation of relapse and survival with amplification of the HER-2/neu oncogene. Science. 1987;235(4785):177-82.
8. Ross JS, Slodkowska EA, Symmans WF, Pusztai L, Ravdin PM, Hortobagyi GN. The HER-2 receptor and breast cancer: ten years of targeted anti-HER-2 therapy and personalized medicine. Oncologist. 2009;14(4):320-68.
9. Dieci MV, Miglietta F, Griguolo G, Guarneri V. Biomarkers for HER2-positive metastatic breast cancer: Beyond hormone receptors. Cancer Treat Rev. 2020;88:102064.
10. Klocker EV, Suppan C. Biomarkers in Her2- Positive Disease. Breast Care (Basel). 2020;15(6):586-93.
11. Triulzi T, Bianchi GV, Tagliabue E. Predictive biomarkers in the treatment of HER2-positive breast cancer: an ongoing challenge. Future Oncol. 2016;12(11):1413-28.

12. Slamon DJ, Leyland-Jones B, Shak S, Fuchs H, Paton V, Bajamonde A, et al. Use of chemotherapy plus a monoclonal antibody against HER2 for metastatic breast cancer that overexpresses HER2. N Engl J Med. 2001;344(11):783-92.
13. Viani GA, Afonso SL, Stefano EJ, De Fendi LI, Soares FV. Adjuvant trastuzumab in the treatment of her-2-positive early breast cancer: a meta-analysis of published randomized trials. BMC Cancer. 2007;7:153.
14. Tinoco G, Warsch S, Gluck S, Avancha K, Montero AJ. Treating breast cancer in the 21st century: emerging biological therapies. J Cancer. 2013;4(2):117-32.
15. Wolff AC, Hammond MEH, Allison KH, Harvey BE, Mangu PB, Bartlett JMS, et al. Human Epidermal Growth Factor Receptor 2 Testing in Breast Cancer: American Society of Clinical Oncology/College of American Pathologists Clinical Practice Guideline Focused Update. J Clin Oncol. 2018;36(20):2105-22.
16. Seol H, Lee HJ, Choi Y, Lee HE, Kim YJ, Kim JH, et al. Intratumoral heterogeneity of HER2 gene amplification in breast cancer: its clinicopathological significance. Mod Pathol. 2012;25(7):938-48.
17. Ohlschlegel C, Zahel K, Kradolfer D, Hell M, Jochum W. HER2 genetic heterogeneity in breast carcinoma. J Clin Pathol. 2011;64(12):1112-6.
18. Hou Y, Nitta H, Wei L, Banks PM, Portier B, Parwani AV, et al. HER2 intratumoral heterogeneity is independently associated with incomplete response to anti-HER2 neoadjuvant chemotherapy in HER2-positive breast carcinoma. Breast Cancer Res Treat. 2017;166(2):447-57.
19. Hanna WM, Ruschoff J, Bilous M, Coudry RA, Dowsett M, Osamura RY, et al. HER2 in situ hybridization in breast cancer: clinical implications of polysomy 17 and genetic heterogeneity. Mod Pathol. 2014;27(1):4-18.
20. Perez EA, Dueck AC, McCullough AE, Reinholz MM, Tenner KS, Davidson NE, et al. Predictability of adjuvant trastuzumab

benefit in N9831 patients using the ASCO/CAP HER2-positivity criteria. J Natl Cancer Inst. 2012;104(2):159-62.
21. Wolff AC, Hammond ME, Schwartz JN, Hagerty KL, Allred DC, Cote RJ, et al. American Society of Clinical Oncology/College of American Pathologists guideline recommendations for human epidermal growth factor receptor 2 testing in breast cancer. Arch Pathol Lab Med. 2007;131(1):18-43.
22. Wolff AC, Hammond ME, Hicks DG, Dowsett M, McShane LM, Allison KH, et al. Recommendations for human epidermal growth factor receptor 2 testing in breast cancer: American Society of Clinical Oncology/College of American Pathologists clinical practice guideline update. J Clin Oncol. 2013;31(31):3997-4013.
23. Chang MC, Malowany JI, Mazurkiewicz J, Wood M. 'Genetic heterogeneity' in HER2/neu testing by fluorescence in situ hybridization: a study of 2,522 cases. Mod Pathol. 2012;25(5):683-8.
24. Stanta G, Bonin S. Overview on Clinical Relevance of Intra-Tumor Heterogeneity. Front Med (Lausanne). 2018;5:85.
25. Vance GH, Barry TS, Bloom KJ, Fitzgibbons PL, Hicks DG, Jenkins RB, et al. Genetic heterogeneity in HER2 testing in breast cancer: panel summary and guidelines. Arch Pathol Lab Med. 2009;133(4):611-2.
26. Hsu CY, Li AF, Yang CF, Ho DM. Proposal of modification for the definition of genetic heterogeneity in HER2 testing in breast cancer. Arch Pathol Lab Med. 2010;134(2):162; author reply 3.
27. Bartlett AI, Starczynski J, Robson T, Maclellan A, Campbell FM, van de Velde CJ, et al. Heterogeneous HER2 gene amplification: impact on patient outcome and a clinically relevant definition. Am J Clin Pathol. 2011;136(2):266-74.
28. Layfield LJ, Schmidt RL. HER2/neu gene amplification heterogeneity: the significance of cells with a 3:1 HER2/CEP17 ratio. Appl Immunohistochem Mol Morphol. 2012;20(6):543-9.

29. Liu Y, Ma L, Liu D, Yang Z, Yang C, Hu Z, et al. Impact of polysomy 17 on HER2 testing of invasive breast cancer patients. Int J Clin Exp Pathol. 2014;7(1):163-73.
30. Dushyanthen S, Beavis PA, Savas P, Teo ZL, Zhou C, Mansour M, et al. Relevance of tumor-infiltrating lymphocytes in breast cancer. BMC Med. 2015;13:202.
31. Badr NM, Berditchevski F, Shaaban AM. The Immune Microenvironment in Breast Carcinoma: Predictive and Prognostic Role in the Neoadjuvant Setting. Pathobiology. 2020;87(2):61-74.
32. Denkert C, Loibl S, Noske A, Roller M, Muller BM, Komor M, et al. Tumor-associated lymphocytes as an independent predictor of response to neoadjuvant chemotherapy in breast cancer. J Clin Oncol. 2010;28(1):105-13.
33. Loi S, Sirtaine N, Piette F, Salgado R, Viale G, Van Eenoo F, et al. Prognostic and predictive value of tumor-infiltrating lymphocytes in a phase III randomized adjuvant breast cancer trial in node-positive breast cancer comparing the addition of docetaxel to doxorubicin with doxorubicin-based chemotherapy: BIG 02-98. J Clin Oncol. 2013;31(7):860-7.
34. Rasmusson A, Zilenaite D, Nestarenkaite A, Augulis R, Laurinaviciene A, Ostapenko V, et al. Immunogradient Indicators for Antitumor Response Assessment by Automated Tumor-Stroma Interface Zone Detection. Am J Pathol. 2020;190(6):1309-22.
35. Ali HR, Provenzano E, Dawson SJ, Blows FM, Liu B, Shah M, et al. Association between CD8+ T-cell infiltration and breast cancer survival in 12,439 patients. Ann Oncol. 2014;25(8):1536-43.
36. Xuan GR, Zhang W, Chai PQ. EM algorithms of Gaussian Mixture Model and Hidden Markov Model. Ieee Image Proc. 2001:145-8.
37. Salido M, Tusquets I, Corominas JM, Suarez M, Espinet B, Corzo C, et al. Polysomy of chromosome 17 in breast cancer tumors

showing an overexpression of ERBB2: a study of 175 cases using fluorescence in situ hybridization and immunohistochemistry. Breast Cancer Res. 2005;7(2):R267-73.
38. Plancoulaine B, Laurinaviciene A, Herlin P, Besusparis J, Meskauskas R, Baltrusaityte I, et al. A methodology for comprehensive breast cancer Ki67 labeling index with intra-tumor heterogeneity appraisal based on hexagonal tiling of digital image analysis data. Virchows Arch. 2015.
39. Haralick R, Shanmugam K, Dinstein I. Textural Features for Image Classification. IEEE Trans Syst Man Cybern. 1973;SMC-3:610-21.
40. Laurinavicius A, Plancoulaine B, Rasmusson A, Besusparis J, Augulis R, Meskauskas R, et al. Bimodality of intratumor Ki67 expression is an independent prognostic factor of overall survival in patients with invasive breast carcinoma. Virchows Arch. 2016;468(4):493-502.
41. Budczies J, Klauschen F, Sinn BV, Gyorffy B, Schmitt WD, Darb-Esfahani S, et al. Cutoff Finder: a comprehensive and straightforward Web application enabling rapid biomarker cutoff optimization. PLoS One. 2012;7(12):e51862.
42. Rushing C, Bulusu A, Hurwitz HI, Nixon AB, Pang H. A leave-one-out cross-validation SAS macro for the identification of markers associated with survival. Comput Biol Med. 2015;57:123-9.
43. Radziuviene G, Rasmusson A, Augulis R, Grineviciute RB, Zilenaite D, Laurinaviciene A, et al. Intratumoral Heterogeneity and Immune Response Indicators to Predict Overall Survival in a Retrospective Study of HER2-Borderline (IHC 2+) Breast Cancer Patients. Frontiers in Oncology. 2021;11.
44. Zilenaite D, Rasmusson A, Augulis R, Besusparis J, Laurinaviciene A, Plancoulaine B, et al. Independent Prognostic Value of Intratumoral Heterogeneity and Immune Response Features by Automated Digital Immunohistochemistry Analysis

in Early Hormone Receptor-Positive Breast Carcinoma. Front Oncol. 2020;10:950.
45. Chen Z, Chen X, Zhou E, Chen G, Qian K, Wu X, et al. Intratumoral CD8(+) cytotoxic lymphocyte is a favorable prognostic marker in node-negative breast cancer. PLoS One. 2014;9(4):e95475.
46. Fortis SP, Sofopoulos M, Sotiriadou NN, Haritos C, Vaxevanis CK, Anastasopoulou EA, et al. Differential intratumoral distributions of CD8 and CD163 immune cells as prognostic biomarkers in breast cancer. J Immunother Cancer. 2017;5:39.
47. Sobral-Leite M, Salomon I, Opdam M, Kruger DT, Beelen KJ, van der Noort V, et al. Cancer-immune interactions in ER-positive breast cancers: PI3K pathway alterations and tumor-infiltrating lymphocytes. Breast Cancer Res. 2019;21(1):90.
48. Baker K, Lachapelle J, Zlobec I, Bismar TA, Terracciano L, Foulkes WD. Prognostic significance of CD8+ T lymphocytes in breast cancer depends upon both oestrogen receptor status and histological grade. Histopathology. 2011;58(7):1107-16.
49. Mahmoud SM, Paish EC, Powe DG, Macmillan RD, Grainge MJ, Lee AH, et al. Tumor-infiltrating CD8+ lymphocytes predict clinical outcome in breast cancer. J Clin Oncol. 2011;29(15):1949-55.
50. Denkert C, von Minckwitz G, Darb-Esfahani S, Lederer B, Heppner BI, Weber KE, et al. Tumour-infiltrating lymphocytes and prognosis in different subtypes of breast cancer: a pooled analysis of 3771 patients treated with neoadjuvant therapy. Lancet Oncol. 2018;19(1):40-50.
51. Solinas C, Ceppi M, Lambertini M, Scartozzi M, Buisseret L, Garaud S, et al. Tumor-infiltrating lymphocytes in patients with HER2-positive breast cancer treated with neoadjuvant chemotherapy plus trastuzumab, lapatinib or their combination: A meta-analysis of randomized controlled trials. Cancer Treat Rev. 2017;57:8-15.

52. Salgado R, Denkert C, Campbell C, Savas P, Nuciforo P, Aura C, et al. Tumor-Infiltrating Lymphocytes and Associations With Pathological Complete Response and Event-Free Survival in HER2-Positive Early-Stage Breast Cancer Treated With Lapatinib and Trastuzumab: A Secondary Analysis of the NeoALTTO Trial. JAMA Oncol. 2015;1(4):448-54.
53. Liu S, Lachapelle J, Leung S, Gao D, Foulkes WD, Nielsen TO. CD8+ lymphocyte infiltration is an independent favorable prognostic indicator in basal-like breast cancer. Breast Cancer Res. 2012;14(2):R48.
54. Mao Y, Qu Q, Chen X, Huang O, Wu J, Shen K. The Prognostic Value of Tumor-Infiltrating Lymphocytes in Breast Cancer: A Systematic Review and Meta-Analysis. PLoS One. 2016;11(4):e0152500.

Vilnius University Press
9 Saulėtekio Ave., Building III, LT-10222 Vilnius
Email: info@leidykla.vu.lt, www.leidykla.vu.lt
bookshop.vu.lt, journals.vu.lt
Print run copies 25